SEQUENTIAL PDGF-SIMVASTATIN RELEASE TO PROMOTE DENTOALVEOLAR REGENERATION

CHONG LI YEN

A THESIS SUBMITTED FOR THE DEGREE OF

MASTER OF SCIENCE

FACULTY OF DENTISTRY

NATIONAL UNIVERSITY OF SINGAPORE

2012

Acknowledgement

This research project would not have been possible without the support of many people. I would like to express my gratitude to my supervisor, A/P Chang Po-Chun who was abundantly helpful and offered invaluable assistance and guidance. I sincerely thank to our collaborators, Prof. Wang Chi-Hwa and his postgraduate students, Chenlu Lei and Noel Xu Qing-Xing for assisting the fabrication of microspheres. Without the knowledge and assistance from Prof. Wang and his students, this study would not have been successful. I would also like to appreciate Jason Lim Chu-Shern for supporting me on micro-CT scanning and working with me during weekends. Special thanks also to all my colleagues, Chung Min-Chun, Chien Li-Ying, Ragal Tsai Sheng-Chueh, Marie Miu Mai Jia, Kao Man-Jung and Alex Dovban Seirgo. I will always remember the days we have been working, chatting and hanging together. Not forgetting all the “lunch peeps” members; Carolina Un Lam, Zou Yu, Lu Qi Qi, Li Ming Ming, Wu Hui Zhen for cheering up my laboratory life. I would also like to convey thanks to the Faculty of Dentistry for providing the financial means and laboratory facilities. Last but not least I wish to express my gratitude to my beloved families for their understanding, support and endless love through the duration of my study.

Table of Contents

List of Appendix

List of Abbreviation

aFGF	(acidic fibroblast growth factor)
bFGF	(basic fibroblast growth factor)
BMD	(bone mineral density)
BMP	(bone morphogenetic protein)
BSA	(bovine serum albumin)
BVF	(bone volume fraction)
CEHDA	(coaxial electrohydrodynamic atomization)
Ctrl	(control without microspheres)
DCM	(dichloromethane)
ECM	(extracellular matrix)
EDTA	(ethylenediaminetetraacetic acid)
EE	(encapsulation efficiency)
ELISA	(Enzyme-linked immunosorbent assay)
GTR	(guided tissue regeneration)
HPLC	(high performance liquid chromatography)
IGF	(insulin-like growth factor)
M1	(maxillary first molar)
M2	(maxillary second molar)

Micro-CT	(micro-computed tomography)
PCNA	(proliferating cell nuclear antigen)
PDGF	(platelet-derived growth factor)
PDL	(periodontal ligament)
PDLLA	(Poly-D,L-Lactide Acid)
PLGA	(poly(lactic-co-glycolic acid))
PS	(PDGF-in-core and simvastatin-in-shell)
ROI	(region of interest)
SB	(simvastatin-in-core and BSA-in-shell)
SEM	(scanning electron microscopy)
SP	(simvastatin-in-core and PDGF-in-shell)
TGF-β	(transforming growth factor-beta)
TMD	(tissue mineral density)
TUNEL	(terminal deoxynucleotidyl transferase dUTP nick end-labelling)
UV	(ultraviolet)
XB	(BSA-in-shell)
XP	(PDGF-in-shell)

Publications

International Journal

(1) Chang P.C., Chung M.C., Lei C., **Chong L.Y.**, Wang C.H. (2012). Biocompatibility of PDGF-simvastatin double-walled PLGA (PDLLA) microspheres for dentoalveolar regeneration: A preliminary study. *Journal of Biomedical Materials Research*. J Biomed Mater Res A. 100(11):2970-8.

(2) Chang P.C., Lim L.P., **Chong L.Y.**, Dovban A.S.M., Chien L.Y., Chung M.C., Lei C., Kao M.J., Chen C.H., Chiang H.C., Kuo Y.P., Wang C.H. (2012). PDGF-Simvastatin Delivery Stimulates Osteogenesis in Heat-induced Osteonecrosis. *Journal of Dental Research*. 91(6):618-24.

(3) **Chong L.Y.**, Chien L.Y., Chung M.C., Liang K., Lim J.C., Fu J.H., Wang C.H., Chang P.C. (2013) Controlling the Proliferation and Differentiation Stages to Initiate Periodontal Regeneration. *Connective Tissue Research.* 54(2):101-7.

International Conference (* presenter)

(1) Chung M.C., **Chong L.Y.***, Lei C., Wang C.H., Chang P.C. Fabrication of sequentially released PDGF-simvastatin double-walled PLGA(PDLLA) microspheres. Tissue-Egineering and Regenerative Medicine International Society Asia-Pacific (TERMIS-AP) Chapter Meeting (August 3-5, 2011), Singapore.

(2) Chung M.C., **Chong L.Y.***, Lei C., Wang Y.P., Wang C.H., Chang P.C. Biocompatibility of PDGF-simvastatin double-walled PLGA(PDLLA) microspheres for dentoalveolar regeneration. 25th International Association for Dental Research South-East Asia (IADR-SEA) Division Annual Meeting (October 29-30, 2011), Singapore.

(3) **Chong L.Y.***, Chien L.Y., Chung M.C., Liang K., Lim J.C., Wang C.H., Chang P.C. Dominant roles of mitogenesis in periodontal regeneration. International Association for Dental Research Singapore Section (IADR-SS) Meeting (October 29-20, 2011), Singapore.

(4) **Chong L.Y.***, Dovban A.S.M., Lim L.P., Lim J.C., Wang C.H., Chang P.C. Sequential PDGF-simvastatin promotes dentoalveolar regeneration. 26th International Association for Dental Research South-East Asia (IADR-SEA) Division Annual Meeting (November 3-4, 2012), Hong Kong.

Abstract

Dentoalveolar regeneration involves a cascade of events regulated by early mitogenic and late-differentiational factors. It is necessary to develop a vehicle delivering multiple bioactive molecules to harmonize mitogenesis and osteogenic differentiation, in order to optimize dentoalveolar regeneration. This thesis aimed at designing and fabricating a delivery system to release platelet derived growth factor (PDGF, mitogen) and simvastatin (osteogenic differentiation promoter) in accordance with cascade of events during regeneration, in order to promote dentoalveolar regeneration in a preclinical model.

To carry the two biomolecules, we utilized a coaxial electrohydrodynamic atomization (CEHDA) technique to fabricate double-walled PLGA (PDLLA) microspheres. The inherent properties of microspheres were characterized by confocal and scanning electronic microscopy, and the encapsulation efficiency, as well as the *in vitro* releasing profile of microspheres, were examined by ELISA and HPLC. For biocompatibility testing, microspheres encapsulating BSA-in-shell (XB), simvastatin-in-core with BSA-in-shell (SB), PDGF-in-shell (XP), simvastatin-in-core with PDGF-in-shell (SP), PDGF-in-core and simvastatin-in-shell (PS), were implanted subcutaneously at the back of rats and examined by histology. For the

regeneration capability, microspheres were filled into critical-sized osseous defects on rat maxillae, and examined by micro-computed tomography (micro-CT) and histology, and defect without any microspheres implantation was designated as control (Ctrl).

The microspheres have rounded morphology with distinct core-shell structure and high encapsulating efficiency. A fast-release of PDGF followed by slow-release of simvastatin was noted in SP-microspheres, whereas PS-microspheres have a parallel release profile. All microspheres demonstrated acceptable biocompatibility *in vivo,* with increased proliferation, reduced apoptosis, and reduced inflammation while PDGF or simvastatin was encapsulated. From the micro-CT assessment, SP-treated-specimens demonstrated highest bone volume fraction (BVF), tissue mineral density (TMD), trabecular thickness, and trabecular number among the groups at day 14. At day 28, elevated BVF, TMD and trabecular number was noted in SB-, XP- and SP-treated-specimens, but not in PS-treated-specimens. Descriptive histology revealed more trabecular bone formation in SP-treated-specimens than the other groups at day 14, and bone maturation was noted in XP- and SP-treated-specimens at day 28.

In conclusion, we successfully fabricated microspheres allowing early release of

PDGF for cell proliferation and delayed release of simvastatin with improved biocompatibility, and the sequential release of PDGF and simvastatin was able to promote dentoalveolar regeneration in a preclinical model.

Chapter 1

INTRODUCTION

Chapter 1:

Introduction

1.1 Periodontal disease: an overview

Periodontal diseases have traditionally been divided into those that involve only gingiva, so-called gingivitis, and those that are associated with the destruction of the underlying structures of the periodontium, so-called periodontitis [1]. The periodontium is referred to as the tooth-supporting apparatus, including gingiva, alveolar bone, periodontal ligament (PDL), and root cementum [1] (Figure 1).

The characteristics of periodontitis are loss of connective tissue, resorption of alveolar bone, and formation of periodontal pockets. It is one of the most common inflammatory diseases in humans, and a leading cause of tooth loss in adults [1-3].

Periodontal disease is caused by specific bacteria in the periodontal pocket [1]. Socransky has developed a classification of oral microorganisms, the so-called Socransky classification. This classification divided the oral microorganisms into five groups based upon the cluster analysis and community ordination, including red,

orange, yellow, green, and purple complexes [4]; where the red complex consists of *Porphyromonas gingivalis, Tannerella forsythia* and *Treponema denticola*, more frequently found in higher numbers in deeper periodontal pockets. The bacteria secretes numerous bacteria products in the periodontal pockets, such as endotoxins, which lead to cytotoxicity [5-7] and collagenase as well as protease, which cause destruction of collagens, proteoglycans and connective-tissue matrix [8, 9]. In addition, bacterial lipopolysaccharide can induce the destruction of bone by a direct effect on bone cells [10, 11]. As a consequence, extensive destruction of the periodontium may finally lead to tooth loss [1].

The current management of periodontal diseases mainly place emphasis on slowing the progression of the disease process, regenerating periodontium, including alveolar bone, periodontal ligament, and root cementum, and preventing recurrence of diseases [12]. The treatment generally starts by establishing excellent oral hygiene, followed by the removal of bacterial plaque and calculus to control inflammation and stop progressive bone loss. In the last two decades, various regenerative procedures have been evaluated to restore the lost periodontium. Among the surgical procedures, the regeneration of damaged periodontal structures with bone graft materials and guided tissue regeneration (GTR) strategies have achieved some success. However, the

outcomes are variable, depending on multiple factors such as defect size and type, patient age and education, genetics, and the operator skills [13, 14]. Some studies demonstrated that these therapies remain limited from both preclinical and clinical studies, especially in terms of cementum and functional PDL regeneration [15-17]. Complete repair and regeneration of functional hybrid periodontal tissues remains an elusive but laudable goal [15, 18]. To date, there is still no ideal therapeutic approach to cure periodontitis or to achieve predictable and optimal periodontal tissue regeneration [18]. The periodontal regeneration rather than repair remains the desired optimal outcome [19-22]. It is anticipated that tissue-engineering methods could overcome some of the limitations associated with the current clinically available strategies [23-26].

1.2 Wound healing cascade

The wound healing cascade takes place in four phases: clot formation, inflammation, proliferation, and maturation [27-30] (Figure 2).

1.2.1 Clot formation

Clot formation is the first step of healing, to stop bleeding and to reduce infection by bacteria, viruses and fungi. The blood clot serves as a provisional matrix for cell

migration and can temporarily protect the denuded tissues [28].

1.2.2 Inflammation

Inflammation takes place within 3 to 24 hours after the wound has been incurred. The inflammatory cells, predominantly neutrophils and monocytes, populate the clotting mechanism. These cells cleanse the wound of bacteria and necrotic tissue through phagocytosis and release of enzymes and toxic oxygen products [31].

1.2.3 Proliferation

Within 3 days, the inflammatory reaction moves into late phase. Macrophages migrate into the wound area and secrete polypeptide mediators targeting cells involved in the wound-healing process for wound debridement. Growth factors and cytokines secreted by macrophages are involved in the proliferation and migration of fibroblasts, endothelial cells, and smooth muscle cells into the wound area [32].

During proliferation phase, immature granulation tissue containing plump active fibroblasts forms. The fibroblasts produce an abundance type III collagen to fill the defect left by an open wound [33].

1.2.4 Maturation

The granulation tissue next undergoes maturation and remodeling. Fibroblasts become more spindle-shape in appearance and produce type I collagen for the replacement of the provisional extracellular matrix. Approximately 1 week following wound healing, some fibroblasts mature into myofibroblasts and express a smooth muscle actin, which enables them to contract and reduce the size of the wound. For angiogenesis, endothelial cells migrate into the provisional wound matrix to form vascular tubes and loops, and as the provisional matrix matures, the redundant vessels formed in granulation tissue are removed by apoptosis, and type III collagen is largely replaced by type I collagen [27, 34].

Maturation of the granulation tissue will lead to the regeneration or repair (scar formation) of the injured tissues. Whether the damaged tissues heal by regeneration or repair depends upon two crucial factors: the availability of cell type(s) needed; and, the presence or absence of cues and signals necessary to recruit and stimulate these cells [17].

1.2.5 Periodontal ligament healing

The periodontal wound healing generally follows the wound healing cascade

mentioned above, and involves periodontal ligament as well as alveolar bone regeneration.

The healing is initialized by the clot formation imposed onto the root surface in a seemingly random manner after treatment. Within minutes, a fibrin clot attached to the root surface is developed. Within hours, inflammatory cells, predominantly neutrophils and monocytes, accumulate on the root surface, and within 3 days the late phase of inflammation dominates the healing process as macrophages migrate into the wound followed by the formation of granulation tissue. At 7 days, collagen fibers adhesion may be seen at the root surface [30]. In about three weeks, the denuded root surface stimulates the differentiation of cementoblasts, which will deposit a hard tissue onto which new collagen fibers may be anchored [35]. Within few weeks of cementum deposition, the resorption on the root surface is initiated. The resorption process establishes a suitable substrate for anchorage of new collagen fibrils [36]. The repaired cementum deposits in the resorbed areas, thus completing the new attachment [37].

1.2.6 Alveolar bone healing

The dynamic of alveolar bone healing was studied by a tooth extraction model in dog [38]. The osteoclastic activity was first noted within 3 days. At 7 days, granulation

tissue was formed. At 14 days, provisional connective tissue and woven bone formation was determined. The woven bone was in a finger-like projection and contained large number of osteoblasts. Bone was continuously undergoing bone remodeling, which was a complex process involving the resorption of bone by osteoclasts, followed by a phase of bone formation by osteoblasts [39]. At 6 months, the woven bone was then replaced by lamellar bone, which has a regular parallel alignment of collagen into sheets and was mechanically stronger than woven bone.

1.2.7 Growth factors involved

Examples of growth factors found locally in bone and healing tissues include platelet-derived growth factor (PDGF), transforming growth factor-beta (TGF-b), acidic fibroblast growth factor (aFGF), basic fibroblast growth factor (bFGF), insulin-like growth factors (IGF-I and IGF-II), and the bone morphogenetic proteins (BMPs) [40]. The PDGF is a potent mitogen and chemoattractant for many cell types, such as fibroblasts and osteoblasts [41]. The actual maturation of the bone from disorganized woven bone into a mature lamellar bone involves IGF and BMP [42].

1.3 Current regeneration approaches

The currently established treatment of periodontal defects including guided tissue

regeneration, bone grafts and bioactive molecules-driven regeneration [43].

1.3.1 Guided tissue regeneration (GTR)

The clinical applications of GTR in periodontics involve the placement of a cell-impermeable barrier membrane between detoxified root surface and the crevicular epithelium in order to enable the repopulation of cells from the periodontal ligament to the root surface [44]. The principle of GTR and its achievements in both preclinical and clinical trials over the past three decades have been comprehensively reviewed [13, 45-48]. Normally, the periodontal defect, if left empty after open flap debridement, will fill with epithelial cells and fibroblasts, which generates a core of fibro-epithelial tissues that ultimately prevent the sequential regeneration of true periodontal tissue. The GTR technique therefore employs a barrier membrane to prevent epithelium down growth and allow fibroblast migration into the wound area, thereby also maintaining the space for target periodontal tissue regeneration [45, 46, 48].

GTR has been applied in many clinical trials for the treatment of various periodontal defects, such as intrabony defects [49], furcation involvement [50, 51] and localized gingival recession [52], and it has become an acceptable procedure in most

periodontal practices today. Indeed, histological analysis of GTR-mediated healing demonstrates that new connective tissue attachment to the root surface forms with minor contributions from new cementum and bone formation, which, by definition, is not true periodontal tissue regeneration. As a result, it is still difficult to draw general conclusions about the clinical benefits of GTR with the currently available and limited evidence.

1.3.2 Bone grafts

Bone grafts aim to restore the height of the alveolar bone around a previously diseased tooth. It was believed that growth factors in the graft were able to release into the implanted area to promote the wound healing and tissue regeneration. In general, there are three types of bone grafts; autogenic, allogenic and xenogenic grafts. A number of reviews have already summarized the advantages and disadvantages of different grafts as well as bone substitutes [13, 53, 54].

Currently, autogenously harvested bone grafts are most commonly used for the replacement of bone material in bone-repair-related research, especially due to the absence of the immunogenic reaction post-surgically. Disadvantages with the use of fresh autogenous grafts include root resorption (iliac crest grafts) and the requirement

for an additional invasive surgical procedure that may result in donor-site morbidity, chronic postoperative pain, hypersensitivity and infection.

Allogenic and xenogenic grafts are widely available and do not require a second surgical site for the patient to harvest autogenous bone. However, allogenic and xenogenic grafts will increase the risks of immunological reactions. In this regard, the grafts must undergo processing techniques such as lyophilization, irradiation or freeze-drying to remove all immunogenic proteins. As a consequence, the osteoinductive and osteoconductive potentials of allografts and xenografts will be decreased as compared with autografts [55].

1.3.3 Bioactive molecules-driven regeneration

Wound healing is regulated by a complex signaling network involving numerous growth factors, cytokines, and chemokines. The application of morphogenetic or mitogenic growth factors to support bone formation at localized alveolar ridge defects has become an area of increasing interest [56]. The currently used bioactive molecules in periodontal diseases include PDGF (GEM 21S, Osteohealth, Shirley, NY, USA), BMP and enamel matrix derivatives (Emdogain, Straumann, Andover, MA, USA). On the other hand, simvastatin, an anti-hyperlipidemia drug, was found to induce osteoblast differentiation and thus becomes a promising biomolecule for

dentoalveolar regeneration.

1.3.3.1 Platelet-derived growth factors in periodontal bone regeneration

Within the family of growth factors, platelet derived growth factor (PDGF) is the class of proteins that has been extensively investigated particularly with reference to the regeneration of periodontal tissues [57-61]. The PDGF receptor signaling has been reported to play an important role in the regulation of proliferation and migration of cells including osteoblasts and fibroblasts [62, 63]. It has been reported that PDGF-BB stimulates the proliferation of osteoblasts and fibroblasts [64, 65].

In the study on beagle dogs, Lynch *et al.* [66] showed that the PDGF promotes new bone formation around periodontal bony defects. The results also demonstrated a continuous layer of osteoblasts lining the newly formed bone in the sites treated with PDGF compared to the sites without PDGF treatment [66]. Since then, several clinical [59-63, 67] and experimental studies [68-72] have been performed to investigate the potency of PDGF in the treatment of periodontal bony defects.

Simion *et al.* found that rhPDGF-BB-infused matrix significantly enhanced bone formation and gingival healing in large, critical-size alveolar bone defects in a dog

model [70]. The rhPDGF-BB was found to exert a potent chemotactic effect on osteogenic cells present in the periostium.

In addition, Schwarz *et al.* conducted a preclinical study to evaluate the healing outcomes following horizontal ridge augmentation [69]. The rhPDGF-BB treated group demonstrated better results in terms of mineralized tissue and total augmented area at 3 weeks than the control group. Taken together, the promising preclinical evidence of PDGF therapy established the foundation for therapeutic evaluation of PDGF in clinical applications.

An early human clinical trial to evaluate the effect of rhPDGF/IGF treatment applied to osseous periodontal defects was reported by Howell *et al*. [59]. The experimental sites received direct application of the growth factors contained in a methylcellulose matrix to improve retention. At nine months post-surgery, the growth-factor-treated sites showed a statistically significant increase in alveolar bone formation as compared with untreated control sites. Average bone height for the PDGF/IGF group was 2.08 mm and 43.2% osseous defect fill was achieved, as compared with 0.75 mm new bone height and 18.5% fill for the control sites.

Recently, a clinical study conducted by Nevins *et al.* had demonstrated that the use of purified recombinant human platelet-derived growth factor (rhPDGF-BB) was safe and effective in the treatment of periodontal osseous defects in patients [61]. The study found that treatment with rhPDGF-BB stimulated a significant increase in the rate of clinical attachment level gain, reduced gingival recession at 3 months post-surgery, and improved bone fill as compared to a β-TCP bone substitute at 6 months. The PDGF has also been used for the bone regeneration around the dental implants [57].

1.3.3.2 Simvastatin in bone regeneration

Simvastatin, a specific competitive inhibitor of 3-hydroxy-2-methyl-glutaryl coenzyme A (HMG-CoA) reductase, is a widely-used anti-hyperlipidemia drug [73, 74]. In recent years, the effect of simvastatin on bone tissue has received particular attention. Mundy *et al.* first reported that simvastatin stimulated *in vivo* bone formation in rodents and increased new bone volume in cultures from mouse calvaria [75]. Several studies further demonstrated that simvastatin is able to modulate bone formation by increasing the expression of BMP-2 and angiogenesis on mouse calvaria and rat mandibles [75-79], providing a new direction in the field of periodontal therapy. Jadhav SB *et al.* found that simvastatin has the ability to initiate osteogenic

differentiation pathway [80], thus considered to promote osteogenesis in the later stage of bone regeneration. Recently, simvastatin was found to support BMP-2-induced osteoblast differentiation through antagonizing TNF-α-to-MAPK pathway and augmenting Ras/Smad/Erk/BMP-2 signaling pathway [81-83].

Simvastatin is shown to increase cancellous bone volume, bone formation rate, and cancellous bone compressive strength *in vivo* [84]. Various animal studies showed that simvastatin assists in bone regeneration, minimizes alveolar bone loss and has protective features against the impact of periodontitis on attachment apparatus and alveolar bone when delivered or applied locally [78, 85-88]. The successful use of simvastatin to promote bone formation *in vivo* depends on the local concentration, and there have been persistent efforts to find an appropriate delivery system [89].

A clinical trial using simvastatin on patients with chronic periodontitis showed that there was a greater decrease in gingival index and probing depth, and more clinical attachment level gain with significant intrabony defect fill at sites treated with scaling and root planning, plus locally delivered simvastatin in patients with chronic periodontitis [90].

1.4 The tissue engineering scaffold

Drug delivery systems are designed in order to enable the growth factor to efficiently exert its biological effects [91, 92]. Current delivery systems still suffer from several limitations for clinical periodontal applications such as loss of bioactivity, limited control over dose administration, nontargeted delivery, and/or lack of availability. The development of a suitable scaffold to overcome these limitations is still needed.

It is well established that cells reside, proliferate, and differentiate inside the body with a complex 3D environment, indicating that an extracellular matrix (ECM) is a pivotal factor with a significant role in supporting or restoring periodontal regeneration.

An artificial ECM, carried out by scaffolding materials, therefore is a prerequisite of most tissue regeneration strategies. Scaffolds are porous, degradable structures fabricated from either natural materials (collagen [93-96], fibrin [97, 98], or synthetic polymers [99-101]). Scaffolds can be sponge-like sheets, gels, micro/nano-spheres, or highly complex structures with intricate networks of pores and channels fabricated using new material-processing technologies. Virtually all scaffolds used in tissue engineering are intended to degrade slowly after implantation in the patient, being

replaced by new tissue [102].

To achieve the functions of a scaffold in tissue engineering, the scaffold should meet a number of requirements, such as interconnected micropores for cell migration and ingrowth, optimal porosity with adequate surface area and mechanical strength, and controlled absorption kinetics or degradation [97, 98, 100, 103].

1.5 Towards the delivery of multiple growth factors

Reconstructive strategies do not always yield satisfactory outcomes [104]. The basis for tissue regeneration is the utilization of engineering techniques that mimic the wound healing cascade, by providing suitable biochemical and physico-chemical factors [105, 106]. Since the wound healing cascade was discovered, it is currently accepted that the self-healing capacity of patients can be augmented by artificially accelerating the proliferation and differentiation of the recruited or implanted cells via the integration of growth factors and cytokines [105-108]. To achieve this goal, it is indispensable to provide cells with a local biochemical and mechanical niche mimicking the natural environment in which they can proliferate and differentiate efficiently by creating an artificial ECM and/or by delivering growth factors [25, 105-110].

With an improved understanding of the critical pathways involved in the development of integrated tissues, the role of growth factors in the wound healing cascade, and the expansion of their availability through recombinant technologies, the use of growth factors is an increasingly important strategy to repair or regenerate damaged/ diseased tissue and is a leading component of tissue engineering approaches [108, 111, 112]. To be effective as a therapeutic agent, a growth factor has to reach the site of injury without degradation, and then, it has to remain in the target location sufficiently long to exert its action(s) [25]. Growth factors that are provided exogenously in solution into the site to be regenerated are generally not effective because growth factors tend to diffuse away from wound locations and are enzymatically digested or deactivated [25, 105-110]. There is increasing evidence that enabling growth factors to exert their biological function efficiently in tissue engineering requires the design and development of release technologies that provide controlled spatiotemporal delivery of key signaling molecules, and prevent unwanted and potentially harmful side-effects [113].

The understanding of the critical pathways in tissues development is leading to guidance on the administration of growth factors, for example, which factors to

deliver and the dose and timing of delivery, for the regeneration of a number of homologous tissues [104]. In the natural wound healing process, responding cells are regulated by a coordinated cascade of events with several growth factors and signaling molecules in a time- and concentration-dependent fashion, which has been clearly established for bone repair [114-117]. This suggests that appropriate presentation of multiple regulatory signals may be a prerequisite for effective tissue engineering strategies; thus, controlled delivery of various combinations of growth factors is a compelling method for the future [104].

Although the delivery of single growth factor has been well-studied, the strategies involved in delivery of two or more growth factors have not been as extensively examined [113]. Research on this concept has begun to harness advances in biomaterials and basic biology to yield next generation medical devices to replace tissue function and new treatment approaches to stimulate or augment endogenous repair mechanisms [104]. Appropriately designed release technology may in turn reduce the amount of protein required to achieve a desired effect, which essentially increases the potency of the growth factors in some cases [111, 112, 118, 119]. The incorporation of multiple growth factors into cell-based tissue engineering systems, therefore, maybe a promising approach for more efficient and effective tissue

regeneration [113]. Since the first attempt of dual growth factors delivery through a polymeric system by Richardson *et al.* [120] concerted efforts have been and still are being made to achieve this ambitious purpose [113].

Chapter 2

HYPOTHESIS AND OBJECTIVES

Chapter 2:

Hypothesis and Objectives

2.1 The hypothesis of this study

The study was designed to test the following hypothesis:

By mimicking the physiological events during wound healing, the combination of the fast release of PDGF and the slow release of simvastatin will promote dentoalveolar regeneration.

2.2 The objectives of this study

The detailed objectives of this study are as following:

(1) To fabricate a delivery system to control release PDGF and simvastatin.

The CEHDA technique was used to fabricate double-walled polymeric microspheres in order to carry PDGF and simvastatin to achieve the release profile in accordance with the physiological events [121] (i.e., fast release profile of PDGF to promote early mitogenesis, and slow release profile of simvastatin to promote later osteogenic differentiation).

(2) To examine the biocompatability of the fabricated microspheres.

The microspheres were implanted subcutaneously and the cell viability (i.e. inflammation, proliferation and apoptosis), as well as the thickness of fibrotic tissue was examined by immunohistochemistry.

(3) To investigate the regenerative ability of fabricated microspheres in a preclinical osseous defect model.

A critical-size bony defect was created on the rat maxilla and filled with (XB, SB, XP, PS, and SP) or without microspheres. The outcome of regeneration was evaluated through descriptive histology and volumetric analysis from micro-computed tomography (micro-CT) data with 6 parameters (bone volume fraction, bone mineral density, tissue mineral density, trabecular thickness, trabecular number and trabecular separation).

Chapter 3

MATERIALS AND METHODS

Chapter 3:

Materials and Methods

3.1 Fabrication of microspheres

3.1.1 The protocol of microspheres fabrication

The microspheres of distinct core/shell structures were fabricated by coaxial electrohydrodynamic atomization (CEHDA) technique in a disinfected hood. The schematic diagram of the set-up of CEHDA is shown in Figure 3.

Briefly, the microspheres with the core-shell structure were respectively made up of 10% PDLLA (M_w = 24,300-75,000) and 10% PLGA (50:50, M_w = 31,300-43,500) (Lactel Absorbable Polymers, Pelham, AL, USA) in dichloromethane solution (DCM, Tedia, Fairfield, OH, USA). As for loading of the biomolecules, 1 mg simvastatin (Pharmaceutical Simtin®-20, National University Hospital of Singapore, Singapore) (hydrophobic agent) was dissolved in corresponding matrix. Meanwhile, the hydrophilic agent, PDGF-BB (Luitpold Pharmaceuticals, Inc., Wilmington, USA) or bovine serum albumin (BSA, Sigma-Aldrich Corporation, St. Louis, MO, USA) was firstly dissolved in DI water and added to the core or shell phase. The mixture was sonicated at 20-30% amplitude for about 60 s with Sonics Vibra cell to form an

emulsion, and the effectiveness was controlled by the amplitude of oscillation of an ultrasonic transducer. Loaded solutions were then transferred to syringes connected with the coaxial needle (Popper and Sons, Lake Success, NY, USA), which is made of 316L stainless steel. The outer capillary has an outer diameter of 0.72 mm and an inner diameter of 0.50 mm. The inner capillary has an outer diameter of 0.40 mm and an inner diameter of 0.20 mm. The spraying process was pre-tested and monitored to confirm that the emulsion is still stable during this process. Two programmable syringe pumps (KD Scientific, Holliston, MA, USA) were used to inject core and shell phase solutions at a specific rate into the inner and outer capillary of the coaxial needle. A voltage generator (Glassman High Voltage Inc., High Bridge, NJ, USA) supplies a high voltage to the nozzle via a crocodile clip. In order to stabilize the electric field around the nozzle, another high voltage is applied to the ring (5 cm in diameter) surrounding the nozzle. The nozzle voltage was fixed at 6.5 kV while the ring voltage was maintained at 3.5 kV, and the flow rates for the core and shell phases were maintained at 1.8 and 2 mL/h respectively. The resultant microspheres collected on the aluminum foil were then maintained in a freeze-dryer for 3 days. In order to visually differentiate the core and shell structure, a fluorescent dye coumarin 6 (Sigma-Aldrich Corporation, St. Louis, MO, USA) was added only in the shell matrix.

3.1.2 Characterization of microspheres

The size and surface morphology of fabricated microspheres were examined by scanning electron microscopy (SEM) (JSM 5600LV, JEOL Technics Co. Ltd, Tokyo, Japan), and the analysis of particle diameter was done by SMILEView software (Bioprecision Diagnostics Ltd, Somerset, UK) at n>50. Confocal laser scanning microscope (Zeiss LSM 510) was employed to observe the distribution of coumarin 6 in microspheres. The dye distribution can be used as an indicator of the extent of mixing of the inner and outer flows at the tip of the coaxial needle.

3.1.3 Encapsulation efficiency and *in vitro* release

To determine the encapsulation efficiency of simvastatin and PDGF or BSA in microspheres, 20.0 mg of double-walled microspheres were dissolved in 1.0 mL DCM and subsequently 1.0 mL fresh PBS was added, vortexed, and centrifuged at 9,000 rpm for 20 min. The aqueous layer was collected, and two more extraction cycles were again performed to maximize the extraction efficiency. PDGF or BSA concentration in aqueous phase and the simvastatin concentration in organic phase were determined by ELISA (R&D system, Minneapolis, MN, USA), Micro BCA protein assay kit (Pierce Chemical, Rockford, IL) and by high performance liquid chromatography (HPLC, HP1200, Agilent Technologies, Palo Alto, CA, USA),

respectively. For the HPLC analysis, extracted simvastatin was reconstituted in mobile phase (70% acetonitrile) and filtered through a 0.22 μm syringe filter. A reverse-phase Poroshell 120 column (EC-C18, 4.6×75 mm, 2.7 μm) was used at a flow rate of 2 mL/min. 10 μL of sample was injected by an auto-sampler and the column effluent was detected at 238 nm with a UV/Vis detector.

For *in vitro* release test, 50.0 mg core/shell microspheres was loaded in 10.0 mL of PBS (pH 7.4) containing 0.05% of Tween 80. The whole system was then placed in an orbital shaker bath (GFL® 1092, Burgwedel, Germany) maintained at 37°C and 120 rpm. At 1, 3, 5, 7, 10 and 14 days, 8.0 mL of the incubated medium was withdrawn and replaced with 8.0 mL of fresh medium. Simvastatin in the resultant release medium was extracted with DCM, and then reconstituted with mobile phase (70% acetonitrile) for HPLC analysis as described above. PDGF and BSA concentration in the resultant release medium were determined by ELISA and Micro BCA protein assay kit, respectively according to the manufacturer's instruction. All the measurements were done in triplicate. This well-established *in vitro* release protocol has been widely used in microsphere drug delivery studies [122], and a previous investigation demonstrated that this *in vitro* release scheme was parallel to the *in vivo* release profile [123].

3.2 *In vivo* biocompatibility

3.2.1 Animal model

Twenty eight-week-old (weight about 300 g) Sprague-Dawley male rats were utilized in this study according to the guidelines of Institutional Animal Care and Use Committee (IACUC) of the National University of Singapore (NUS). All procedures were performed under the generalized coverage of ketamine (70 mg/kg) and xylazine (10 mg/kg), and instruments were sterilized before and after microspheres delivery. Microspheres encapsulating BSA-in-shell (XB), simvastatin-in-core and BSA-in-shell (SB), PDGF-in-shell (XP), PDGF-in-core and simvastatin-in-shell (PS), and simvastatin-in-core and PDGF-in-shell (SP), were sterilized by UV overnight. Each kind of microspheres was randomly inserted subcutaneously in either left or right side of the back of rats respectively (n=4), and the skin wound was closed by using the surgical clips. The rats were sacrificed, and tissues were harvested at day 10 and 14 post-insertion.

3.2.2 Histology assessment

Each implanted area was collected and fixed in 10% formalin for 3 days, then embedded in paraffin, and cut into 5 μm in thickness. Specimens were stained with Heamatoxylin and Eosin (Polysciences, Warrington, PA, USA) for descriptive

histology and quantifications of inflammatory cells and thickness of the fibrotic wall. Inflammatory cells were quantified based on the cellular characteristics in three randomly-selected areas under 400× magnification in each specimen, and the results are presented as the percentage of inflammatory cells to the total amount of cells. The thickness of fibrotic wall was measured from 10 randomly-selected areas under 200× magnification.

Cell viability was assessed by immunohistochemistry, the staining was done by using a Cell & Tissue Staining Kit (R & D Systems, Minneapolis, MN, USA) for the expression of proliferating cell nuclear antigen (PCNA) and TUNEL technology utilizing an *in situ* Cell Death Detection Kit (POD, Roche Applied Science, Basel, Switzerland). Following the blocking of nonspecific binding with serum, the sections were incubated with the following first primary antibodies: anti-proliferating cell nuclear antigen (anti-PCNA, dilution 1:200, Abcam, PLC, Cambridge, UK) and antibody provided in the *in situ* Cell Death Detection Kit (dilution 1:9, Roche Applied Science) overnight at 4°C, and subsequently incubated with the correspondently biotinylated secondary antibodies for 1 h at room temperature. The color were developed by 3,3-diaminobenzidine (DAB), and sections were finally counterstained with hematoxylin after they were applied HRR-Horse-Radish Perioxidase for 30 min.

Quantifications of proliferating and apoptotic cells were performed in three randomly selected areas under 400× magnification in each specimen, and the results are presented as the percentage of cells with positive signals to the total amount of cells. All images were acquired by a Leica DMD108 system (Leica DMD108 system, Leica Microsystems GmbH, Wetzlar, Germany).

3.3 Preclinical Osseous Defect Model and Study Design

3.3.1 Animal model and study design

All animal procedures were performed under the protocol 057/10 approved by the IACUC of NUS. The study design is shown in Figure 4A and an osseous defect model was created to analyze the capability of alveolar bone regeneration (Figure 4B).

The maxillary first molars (M1) of 36 4-week-old male Sprague-Dawley rats were extracted under general anesthesia covered by ketamine (70 mg/kg) and xylazine (10 mg/kg). After 4 weeks of socket wound healing, a critical-sized osseous defect was created in the M1 edentulous ridge next to the mesial aspect of the second molar (M2). Briefly, a 2.0 mm-in-diameter and 1.0 mm-in-depth osteotomy was firstly created in the edentulous ridge using a customized drill. Microspheres encapsulating XB, SB, XP, PS or SP were placed to completely fill the defects and the wound was closed by approximating the gingival tissues and sealed with cyanoacrylate gel (Histoacryl,

TissueSeal, Ann Arbor, MI, USA). We also created a control which without any implantation of microspheres (Ctrl). The animals were sacrificed at 14 or 28 days post-surgery. Maxillae were harvested and fixed in 10% neutral formalin for 3 days, and stored in 70% ethanol for the subsequent micro-CT assessment.

3.3.2 Volumetric micro-CT measurement

Scans were acquired on a Siemens Inveon CT (Siemens Healthcare, Erlangen, Germany) at 2 × 2 binning and high magnification, achieving an ideal dynamic range and an effective voxel size of 19.54 μm. Images were reconstructed with no downsampling, using the Shepp-Logan algorithm and beam-hardening correction as recommended by the manufacturer. Customized software written in MATLAB (Natick, MA, USA) was used to load and segment the image volumes. The region of interest (ROI) was defined as a round area with a diameter of 2.0 mm and a depth of 1.0 mm (Figure 5). The boundary of ROI was identified by the distinct difference of the mineral density, whereby the native bone demonstrated a higher density than the neogenic bone [104]. The ROI was then segmented to the foreground (bone) and background (soft tissue) by a local edge-specific algorithm [104], and the bone volume fraction (BVF, bone area/total area), bone mineral density (BMD), tissue mineral density (TMD), and the trabecular analysis (trabecular thickness, trabecular

number and trabecular separation) of the ROI was calculated using CT-analyzer software (Skyscan, Antwerp, Belgium).

3.3.3 Histology assessment

Specimens were decalcified with 12.5% EDTA (pH7.4) for 3 weeks after micro-CT scanning. Specimens were then embedded in paraffin, cut into 5 μm thickness, and stained with Hematoxylin and Eosin for descriptive histology assessment. All images were acquired by a Leica DMD108 system (Leica DMD108 system, Leica Microsystems GmbH, Wetzlar, Germany).

3.4 Statistical analysis

Statistical analysis was performed utilizing statistical software (GraphPad Software Inc., La Jolla, CA, USA). Data were pooled according to the experimental groups and presented as mean ± standard error of measurements. The differences in micro-CT measurements and quantitative histological analysis were compared by unpaired *t*-tests with a $p < 0.05$ being considered statistically significant.

Chapter 4

RESULTS

Chapter 4:

Results

4.1 Characterization of microspheres

4.1.1 The morphology

The uniform-sized microspheres (18-20 μm in diameter) were successfully fabricated by CEHDA technique (Figure 6). The morphology of microspheres was determined by SEM (Figure 6). The microspheres in each group demonstrated a regular rounded in morphology with a rough surface and porous structure.

4.1.2 The core/shell structure

The core/shell structure of the microspheres was verified by confocal laser scanning microscope (Figure 7). A distinct core-shell structure can be seen under confocal microscopy. The green fluorescent ring-shape shell was seen due to the fluorescent dye coumarin 6 added to the shell solution. No green fluorescence was found in the core area.

4.1.3 Encapsulation efficiency of biomolecules in microspheres

The core/shell structured microspheres with simvastatin (hydrophobic) encapsulated in the core and PDGF (hydrophilic) encapsulated in the shell (SP), and microspheres with PDGF-in-core and simvastatin-in-shell (PS), were successfully fabricated by CEHDA. Concurrently, microspheres encapsulating XB, SB, and XP, were also developed for comparison (Table 1).

As summarized in Table 1, the encapsulation efficiencies (EE) of simvastatin are about 80-90% in both simvastatin-in-core (SB and SP) and simvastatin-in-shell (PS) samples. The EE of PDGF in the PDGF-in-shell samples (XP and SP) is about 60%, whereas in the PDGF-in-core sample (PS) the EE is about 96%. The BSA has a similar EE to PDGF, which is about 60% when BSA encapsulated in the shell (XB and SB sample).

4.1.4 *In vitro* release of biomolecules from microspheres

Sample XB and SB represent a significant initial burst of BSA with more than 50% released within the first 3 days (Figures 8A and B). The release was almost complete in 7 days. In contrast, the initial burst of simvastatin was minimal. Only about 30% of simvastatin was released at day 5, while the cumulative release just achieved

approximately 50% in a 14-day time window. Similar release results were indicated for sample XP and sample SP with PDGF in substitute of BSA (Figures 8C and E). The initial burst of PDGF from sample XP and SP was about 80% at day 7, while the release profile was linear for simvastatin with about 50% being released after 14 days. The sample SP demonstrated sequential PDGF release followed by simvastatin. Compared to sample SP, the release of biomolecules from sample PS was relatively straightforward (Figure 8D). The release profiles of simvastatin and PDGF were well coupled, although the release rate of PDGF is slightly lower than simvastatin from day 3 to day 14. Different from the release pattern of samples SB and SP (Figure 8B and E), the release pattern of PS was classified as a parallel release (Figure 8D).

4.2 Biocompatibility of the microspheres

4.2.1 Descriptive histology

The evaluation on the biocompatibility of microspheres was based on the observed inflammatory and healing responses after implantation [124]. Generally, fibrous tissue encapsulating residual polymers with minimal inflammatory cell infiltrate was noted in all specimens, and increasing cellularity without significant elevation of inflammation was indicated in the specimens with microspheres encapsulating PDGF (i.e., XP-, SP-, and PS-treated-specimens) at day 10 (Figure 9).

At day 14, a mild increased infiltration, predominantly lymphocytes and a few plasma cells, was observed in most specimens (Figure 10), especially in SB-treated-specimens (Figure 10B). Therefore, inflammation appeared to be relieved when combining with PDGF delivery, and significant angiogenesis was noted in both PS- and SP-treated-specimens (Figures 10D and E). No signs of acute inflammation or abscess formation were noted in any of the specimens.

4.2.2 Density of inflammation and cell viability assessment

The biocompatibility was further examined by the density of inflammation and cell viability, including the proliferation profile by PCNA staining, and apoptosis by TUNEL staining. The images of PCNA and TUNEL staining at 10 days after implantation were shown in Figures 11 and 12, respectively. Quantitative measurements revealed that encapsulating bioactive molecules (both simvastatin and PDGF) can achieve a higher percentage of proliferating cells within the implanted site at day 10 (Figure 13). A significant difference of proliferating cells compared to the XB control was noted for SB-, XP-, and SP-treated-specimens, and inflammation was significantly reduced in XP-treated-specimens compared to the XB control (Figure 13). In contrast, the results from TUNEL staining revealed scant distribution of apoptotic cells in all specimens at day 10 (Figure 13).

The images of PCNA and TUNEL staining at 14 days after implantation are shown in Figures 14 and 15, respectively. At day 14, SP-treated-specimens still tended to demonstrate a higher proliferating profile than all of the other groups examined, however, there was no significant difference of proliferating cells between any bioactive molecules-loading group and the control group (Figure 16). The density of inflammation appeared equivalent among all groups (Figure 16). A slightly elevated expression of apoptotic cells were found in the control group, especially compared to XP-treated and PS-treated specimens (Figure 16). Bioactive molecules appeared to reduce cell apoptosis, and PS-treated-specimens demonstrated significantly fewer apoptotic cells than the control at both day 10 and 14 (Figures 13 and 16).

The images of fibrotic wall around the microspheres at 10 and 14 days after implantation were shown in Figures 17 and 18, respectively. The thickness of the fibrotic wall tended to increase in SB-treated-specimens at day 10, but decrease in PS- and SP-treated-specimens at day 14 (Figure 19).

4.3 Preclinical osseous defect study

4.3.1 Volumetric micro-CT assessment

The transverse plane of micro-CT images at 14 and 28 days after surgery were shown

in Figures 20A and B, respectively. The images from the sagittal plane are shown in Figure 21.

At day 14, there was a trend of increasing BVF, TMD, trabecular thickness and trabecular number in XP-, PS- and SP-treated-specimens compared to controls. The BVF of SP-treated specimens was 35.2 ± 17.7 %, which was the highest among the groups and significantly higher than the Ctrl- (7.4 ± 3.9 %, $p < 0.01$) and XB-treated specimens (9.4 ± 4.1 %, $p < 0.01$). The SP-treated specimens demonstrated the highest TMD (328.7 ± 107.4 mg/cc), and was significantly higher than the Ctrl- (206.7 ± 105.8 mg/cc, $p < 0.05$) and XB-treated specimens (165.9 ± 49.9 mg/cc, $p < 0.05$). The trabecular analysis revealed that SP-treated specimens had the highest trabecular thickness (0.23 ± 0.06 mm), and were significantly higher than both Ctrl- (0.16 ± 0.03 mm, $p < 0.01$) and XB-treated specimens (0.18 ± 0.03, $p < 0.05$). The trabecular number in SP-treated specimens was also the highest (1.65 ± 0.34 1/mm) among the groups with statistically significant to the Ctrl- (0.43 ± 0.18 1/mm, $p < 0.001$) and XB-treated specimens (0.51 ± 0.21 1/mm, $p < 0.001$) (Figure 22). PS-treated-specimens demonstrated significantly higher BVF, trabecular thickness and trabecular number than controls. The SB-treated-specimens showed slight increase of BVF, TMD and trabecular number than controls. There was a decreasing

trend of trabecular separation in SP- and PS-treated specimens as compared to controls.

At day 28, elevated BVF, TMD and trabecular number was noted in SB-, XP- and SP-treated-specimens but not in PS-treated-specimens (Figure 23). SP-treated-specimens demonstrated highest BVF (44.5 ± 4.2 %) among the groups and significantly higher than XB-treated specimens (13.9 ± 7.6 %, $p < 0.01$). SB- and XP-treated specimens showed significant increase of BVF (37.5 ± 5.1 % and 44.1 ± 7.6 %, respectively) compared to XB-treated specimens. The PS-treated specimens, however, did not have much increase of BVF at day 28 (32.3 ± 22.1 %). The TMD of SB-, XP- and SP- were 372.2 ± 32.4 mm/cc, 431.2 ± 57.9 mm/cc and 413.1 ± 34.4 mm/cc respectively which were significantly higher than the XB-treated specimens (183.5 ± 60.4 mm/cc, $p < 0.05$). The trabecular thickness was increased in all groups especially in SB-, XP- and SP-treated specimens (0.29 ± 0.06 mm, 0.34 ± 0.06 mm and 0.34 ± 0.03 mm respectively) these were again significantly higher than the XB-treated specimens (0.19 ± 0.06 mm, $p < 0.05$) . SB- and XP-treated specimens demonstrated significant increase of trabecular number (1.3 ± 0.2 1/mm and 1.3 ± 0.4 1/mm respectively, $p < 0.05$). A decreasing trend of trabecular separation was also noted in SB-, XP- and SP-treated specimens.

4.3.2 Descriptive histology

Slight inflammatory cells infiltration was noted in each group at day 14. The front of osteogenesis is shown in Figure 24. Generally, newly-formed trabecular bone were fromed from the border accompanying with polymer residues distributing in the defect. XB-treated specimens demonstrated scanty new bone within the defect, and scatter bone distribution was found in SB-treated specimens. The XP-treated specimens demonstrated slightly more trabecular bone than SB-treated specimens. The PS- and SP-treated specimens revealed more bone formation and higher degree of trabecular thickness than the other groups. In addition, the reversal lines were also noted in the PS- and SP-treated specimens.

At day 28, fewer inflammatory cells were found within the defect. In general, the newly-formed bone became mature with higher trabecular thickness and less trabecular separation (Figure 25). There were cell bundles lining on the newly-formed bone in Ctrl specimens. In XB-treated-specimens, bone formation appeared to be slightly greater than Ctrl specimens. The newly-formed bone in SB-treated-specimens was greatly increased compared to controls (i.e., Ctrl and XB-treated specimns). XP- and SP-treated-specimens demonstrated elevated bone volume and trabecular thickness. Several reversal lines were obviously found in XP- and SP-treated

specimens. The PS-treated-specimens had less newly-formed bone than SB-, XP- and SP-treated-specimens. Moreover, an increase in cell density was noted in PS-treated-specimens.

Chapter 5

DISCUSSION

Chapter 5

Discussion

Regeneration of damaged periodontal tissues is the ultimate goal for periodontal treatment, and delivering local signals in accordance with the dynamics of healing is capable of facilitating the process of regeneration [26]. As the wound repair involves a cascade of events with the coordination of multiple signals [26], combinational release of multiple signals can potentially render a more favorable and predicable therapeutic outcome than single intervention that was currently used.

5.1 Fabrication of microspheres

Since the biomolecules have the nature of fast degradation and diffusion rate *in vivo,* it is necessary to encapsulate the biomolecules in order to modulate those events [119]. In the present study, microspheres were utilized to carry and control the release of PDGF or simvastatin. The CEHDA technique allowed us to encapsulate two different types of biomolecules in one single step. The releasing profile of biomolecules was varied based on the difference of degradation rate of polymer used, configuration of the microsphere, and hydrophilicity of carried molecules. In the present set-up, PDLLA degraded more slowly than PLGA [125], core-loaded

biomolecules released more slowly than shell-loaded one [121], and hydrophobic agent (simvastatin) released more slowly than hydrophilic agent (PDGF) *in vivo*. As a consequence, those properties enabled an early-release profile of PDGF followed by slow-release of simvastatin. On the other hand, by reversing the compartment in the microspheres (PDGF-in-core and simvastatin-in-shell), a parallel release profile of PDGF and simvastatin can be achieved.

As shown in Figure 8, approximately 80% of shell-loaded protein (BSA or PDGF, hydrophilic agent) and 30% of core-loaded biomolecules (simvastatin, hydrophobic agent) were released at day 7. This result was in accordance to the previous study which investigated the release of a hydrophobic drug paclitaxel and a hydrophilic drug suramin from PLGA/PLLA core-shell microspheres [122, 126], whereas the paclitaxel-in-the-core and suramin-in-the-shell microspheres showed a sequential release of suramin followed by paclitaxel, and suramin-in-the-core and paclitaxel-in-the-shell microspheres displayed a parallel release profile. Similar results on the combination of paclitaxel and carboplatin in PLGA/PLLA microspheres were also reported.

5.2 Biocompatibility of microspheres

The basic criteria of implantable material for medical device should be biocompatible, inert and safe [127]. In this sense, investigations for biocompatibility mainly aimed on cell viability and destructive inflammatory profiles [128, 129]. Poly(lactic-acid) and poly(glycolic-acid) are generally degraded by hydrolysis and the degradation products can stimulate transient inflammation and formation of fibrous microcapsules [127]. The inflammation can be reduced by slowing down the degradation rate but will not resolve until the disappearance of the polymer fragments [130]. In the present study herein, only a low-level of inflammation was observed within the implanted area enabling the present microspheres to be suitable for dentoalveolar regeneration (Figures 13 and 16).

XP-treated-specimens demonstrated elevated PCNA expression and reduced cell death (Figure 16), indicating that the PDGF was biologically active and our microspheres were able to support PDGF-mediated cellular activities. Persistent reduction of apoptosis until day 14 implies that PDGF may overcome the tissue reaction elicited by the degradation products of PLGA (PDLLA). It was not surprising that the proliferation recessed at day 14, where more than 80% of PDGF had been released within 10 days (Figure 8).

A reduction of apoptosis and inflammation was also noted in SB-treated-specimens. Studies had indicated that statins may reduce inflammation through the regulation of cellular behavior as well as reduction of inflammatory cytokines [131, 132]. Simvastatin had been demonstrated to perform osteoinduction in several *in vitro* studies [75, 133], however, the *in vivo* studies have been limited to the change of quality of bone or osseous wound repair models [87, 134, 135]. In this study, simvastatin was subcutaneously implanted and the results revealed that simvastatin is unlikely to induce ectopic osteogenesis. This finding was similar to the previous study, which reported that subcutaneous delivery of statins can neither elicit ectopic calcification nor significant toxicity or inflammation [136]. On the other hand, Sugiyama *et al.* [137] reported that BMP-induced ectopic bone formation was augmented in combination with simvastatin. Taken together, simvastatin appears to present an osteopromotive rather than osteoinductive effect *in vivo*. The efficacy should be evaluated with the presence of other osteoinductive factors.

The dual-biomolecules delivery systems (PS- and SP-microspheres) demonstrated further improvement on biocompatibility (Figures 9-19). Specifically, parallel release of PDGF and simvastatin (PS-microspheres) can significantly reduce cell death. This may due to the synergistic effect of simvastatin and PDGF by inhibiting inflammatory

cytokines and upregulating anti-apoptotic signaling pathways, respectively [132]. The SP-treated-specimens demonstrated significant and persistent enhancement of proliferation, indicating the prominent mitogenesis effect of PDGF in early stages, and the subsequent release of simvastatin in later stage can render a suitable environment for angiogenesis and tissue repair, indirectly favoring the growing of mesenchymal and endothelial cells [138].

5.3 *In Vivo* Efficacy

At day 14, generalized osteogenesis was observed in XP-treated specimens, but SB-treated-specimens showed only scattered osteogenesis (Figure 24D). This result could be associated with the promotion of stem cells recruitment and proliferating by PDGF [139]. Due to the lack of molecular signaling for cell recruitment in the early stages of regeneration, only a slight increase in mineralization was noted in the SB-treated specimens. Limited numbers of cells with differentiation capability within the defect could still impede regeneration in the later stage. While the recruitment and mitogenesis of stem cells were the dominant event in the early stage of wound healing [140], fast release of PDGF within the first week of delivery may reasonably augment these events. On the other hand, we also noted that osteogenesis took place close to the SB-loaded microspheres (Figure 24C), presumably due to the direct enhancement

of osteogenesis, via the activation of the Smad pathways and BMP-signaling [82]. In contrast, without direct involvement in BMP-signaling, the distance between the front of osteogenesis and PDGF-loaded microspheres was greater [141] (Figure 24D).

The dual-biomolecules delivery systems (PS- and SP-microspheres) demonstrated further improvement on bone-forming at day 14 (Figure 22). The PS-treated-specimens demonstrated significant increase of newly-formed bone and trabecular number than the control. This may due to the synergetic effect of PDGF on cells recruitment and proliferation [139] and the induction of cells differentiation by simvastatin [80]. The SP-treated-specimens showed the highest increase in newly-formed bone, trabecular thickness and trabecular number. This indicated that sequential release of PDGF and simvastatin can further improve bone regeneration due to timely augmentation of proliferation and differentiation by mimicking the physiological events. In a previous study, the combination of PDGF and BMP-7 expressed by adenovirus vectors on chitosan/collagen scaffolds has also demonstrated synergetic bone-forming effects in a dog model [142]. However, sequential release of PDGF and BMP-7 was not investigated in this study. In this study, we used simvastatin, a clinical drug, to replace the differentiation factor, BMP. The double-walled microspheres were utilized for the ease of controlling the releasing rate

of two biomolecules with a desire profile.

At day 28, elevated bone growth was noted in SB- and XP-treated-specimens (Figures 23 and 25). This may due to gradually increase of progenitor cells and endogenous signals within the defect at the later stage. Since PDGF is not directly involved in osteogenic differentiation, the osteogenesis in XP-treated-specimens was only promoted at day 28. On the other hand, simvastatin promoted osteogenic differentiation with limited effects on cell recruitment, the osteogenesis of simvastatin treatment was limited at the early stage. The SP-treated-specimens demonstrated nearly 40% of bone growth whereas limited bone formation was found in the PS-treated-specimens (Figures 23 and 25). This revealed that parallel release of PDGF and simvastatin may prevent subsequent bone growth at the later stage. Given that PDGF did not elicit the differentiation potential of cells, and consistent expression of PDGF may prevent stem cells from differentiation and retard the maturation of bone [143, 144], tissue mineralization might remain primitive and limited in the later stage if PDGF was still in effect. Due to the minimal level of PDGF in the SP-treated-specimens in later stages, the inhibition of osteogenesis could be prevented, leading to continuous bone growth and maturation at day 28.

Chapter 6

CONCLUSIONS AND FUTURE PERSPECTIVE

Chapter 6

Conclusions and Future Perspective

6.1 Conclusions

1. We successfully fabricated double-walled microspheres which sequentially released PDGF and simvastatin when encapsulated PDGF in the shell and simvastatin in the core. Moreover, parallel released of PDGF and simvastatin can also be achieved by encapsulating PDGF in the core and simvastatin in the shell.

2. The fabricated microspheres were biocompatible and biologically active.

3. Sequential PDGF and simvastatin can promote dentoalveolar bone formation and maturation in the preclinical model.

6.2 Future perspective

Although PDGF was delivered to promote cell proliferation and recruitment, local stem cells may be damaged or lack the ability to differentiate into osteogenic cells in the defects. In this regard, providing exogenous cells may be needed [145, 146]. Thus,

combination of exogenous cells with controlled bioactive molecules releasing profiles could be considered to further optimize the outcome of regeneration [142]. On the other hand, according to that PDGF and simvastatin had been FDA-approved and available for clinical use in Singapore, further investigations in large animals or early human trials are indicated.

Chapter 7

APPENDIX

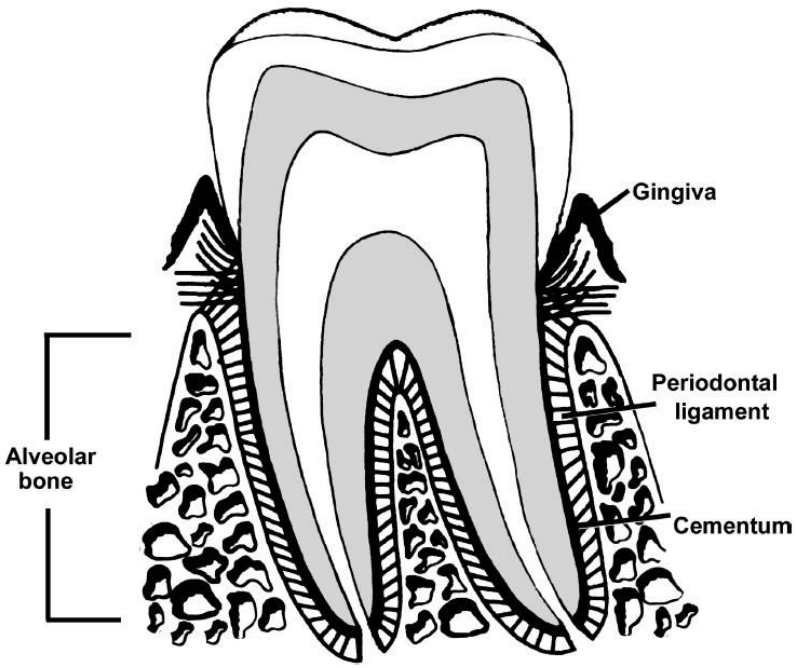

Figure 1. Schematic illustration of the tooth-supporting apparatus in normal periodontium.

The normal periodontium comprised of gingiva, alveolar bone, cementum, and periodontal ligament (PDL). *Adapted from [43]*

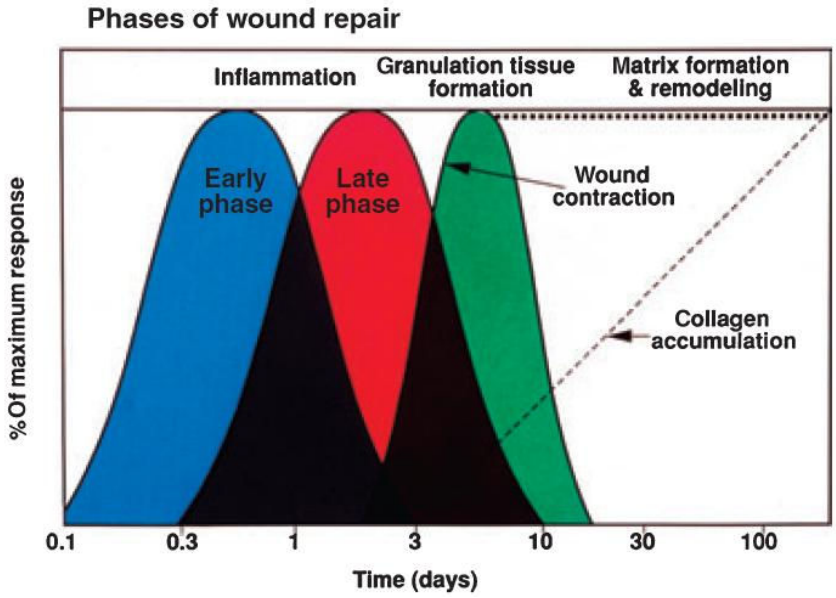

Figure 2. Phases of wound healing.

Adapted from [30]

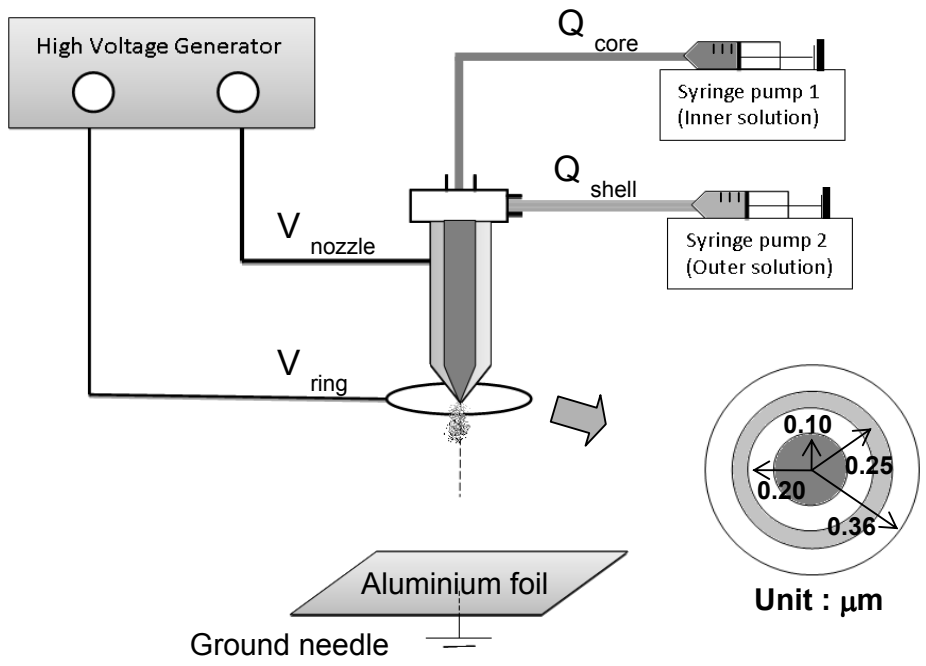

Figure 3. Schematic diagram of the coaxial electrohydrodynamic atomization technique.

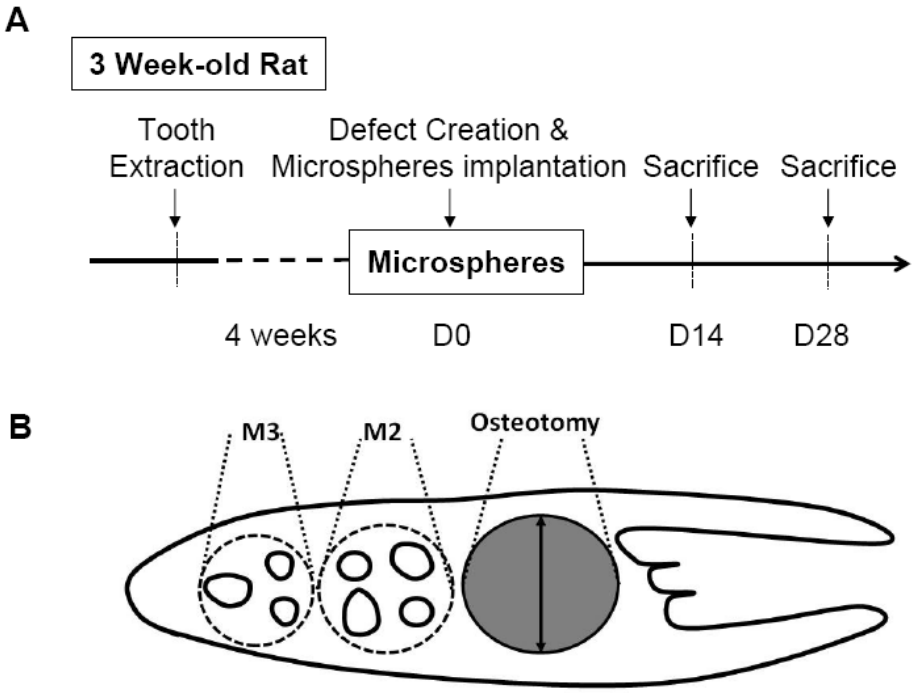

Figure 4. Animal study design and defect creation

(A) The study design. Critical-sized osseous defects was created after 4 weeks of socket wound healing and filled with microspheres (encapsulating XB, SB, XP, PS and SP). The maxillae were extracted after 14 (D14) and 28 days (D28) of microspheres filling. **(B)** The osseous defect created in the edentulous ridge after the extraction of maxillary first molar (M1).
Abbreviations: M2: second molar; M3: third molar.

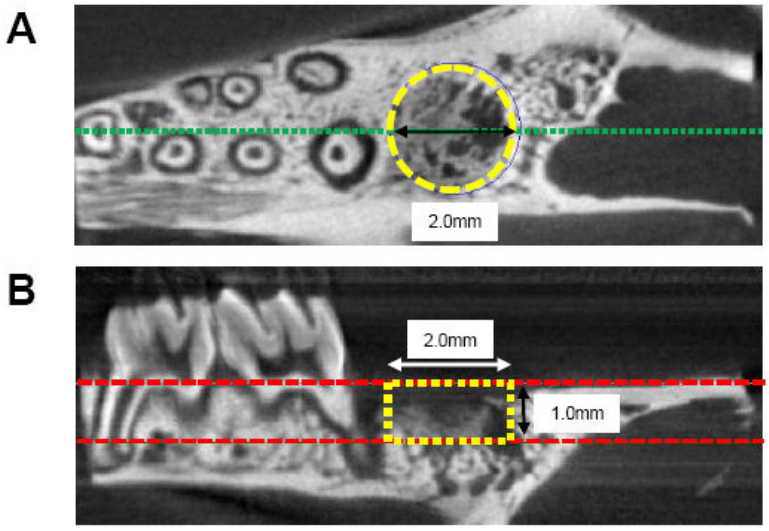

Figure 5. The selection of ROI for quantitative micro-CT measurement.

(A) The transverse plane. Yellow dash line indicates the ROI. Native bone and newly-formed bone. **(B) The sagittal plane**. After selection of ROI from transverse plane, a horizontal line (red dotted line) was drawn at the sagittal plane according to the edge of the alveolar bone around the defect and a vertically 1mm in depth from the edge was automatically selected. The whole stack of ROI will be selected followed by measurement of BVF using a customized MATLAB program.

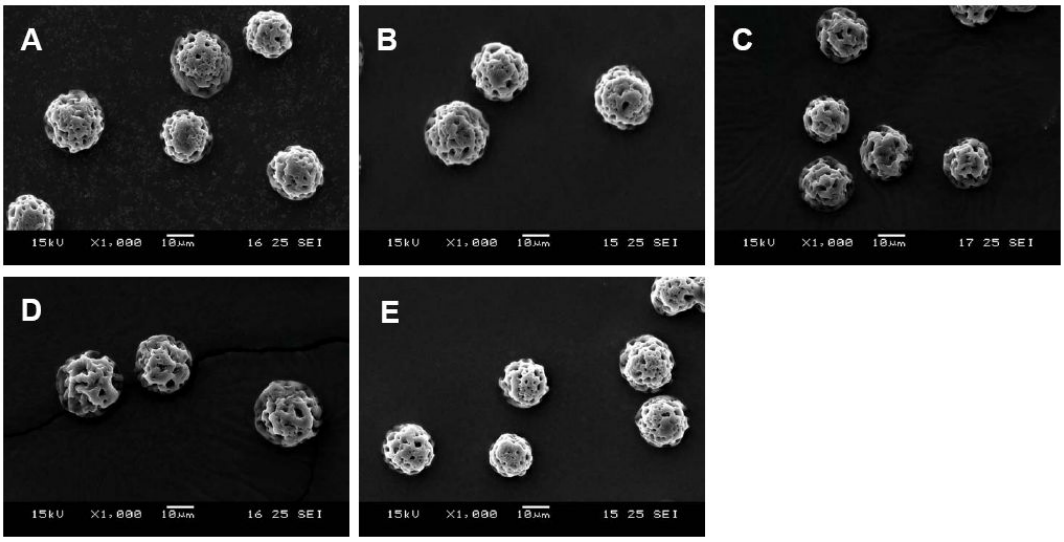

Figure 6. Morphology of double-walled microspheres.

SEM images of microspheres with (A) BSA-in-shell (XB) (B) simvastatin-in-core and BSA-in-shell (SB) (C) PDGF-in-shell (XP) (D) PDGF-in-core and simvastatin-in-shell (PS) (E) simvastatin-in-core and PDGF-in-shell (SP).

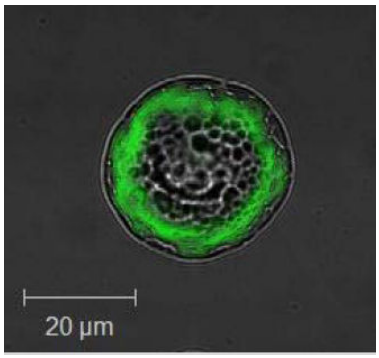

Figure 7. Morphology of double-walled microspheres.

Confocal fluorescence images of core/shell structure microspheres with coumarin 6-stained shell.

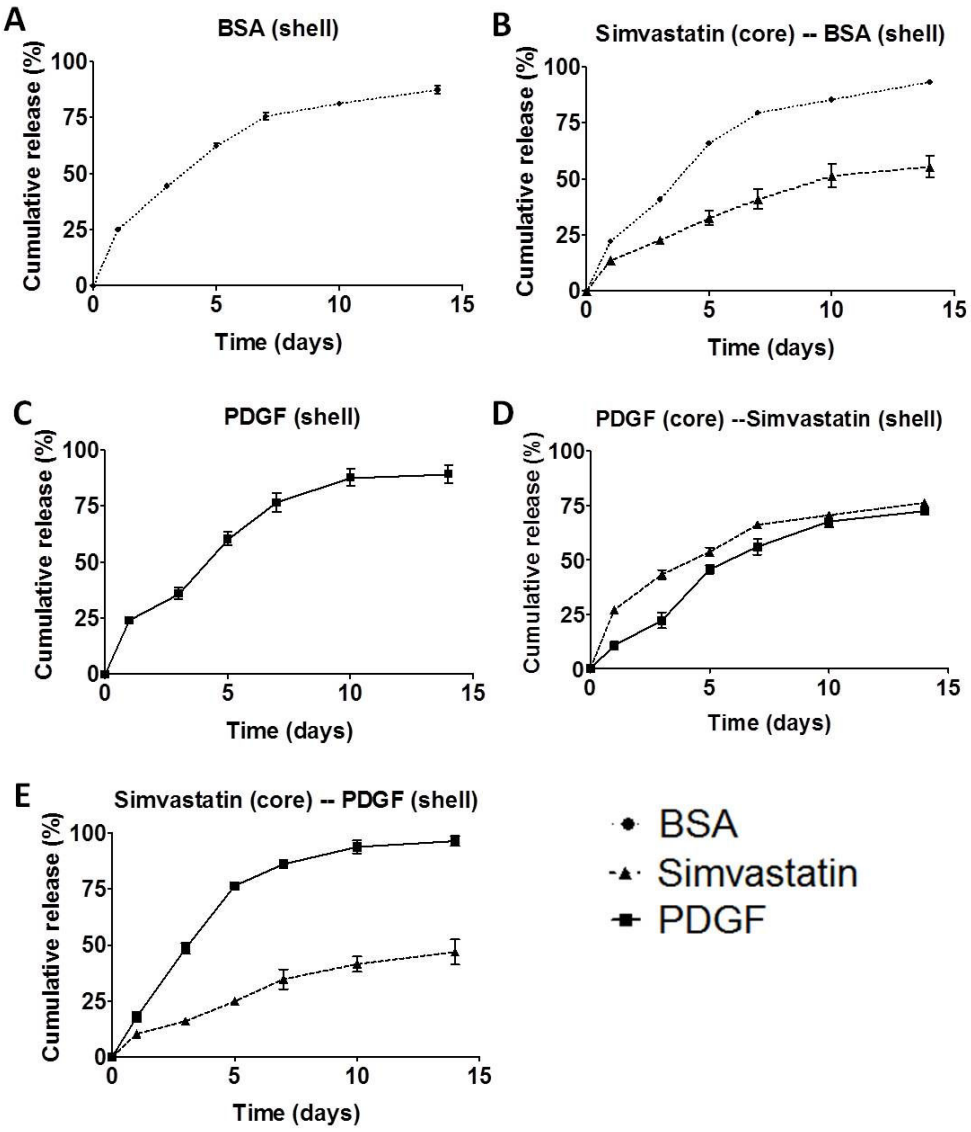

Figure 8. *In vitro* release profile of each group from day 1 to day 14.

Microspheres with (A) BSA-in-shell (XB) (B) simvastatin-in-core and BSA-in-shell (SB) (C) PDGF-in-shell (XP) (D) PDGF-in-core and simvastatin-in-shell (PS) (E) simvastatin-in-core and PDGF-in-shell (SP).

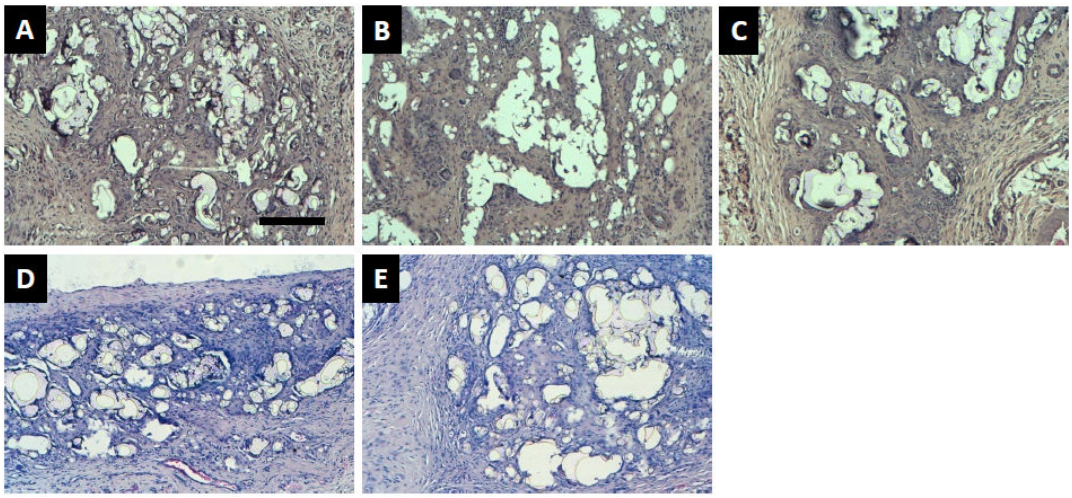

Figure 9. Histology of double-walled microspheres after 10 days implantation, x100.

Microspheres with (A) BSA-in-shell (XB) (B) simvastatin-in-core and BSA-in-shell (SB) (C) PDGF-in-shell (XP) (D) PDGF-in-core and simvastatin-in-shell (PS) (E) simvastatin-in-core and PDGF-in-shell (SP). (Scale bar represents 200 μm.)

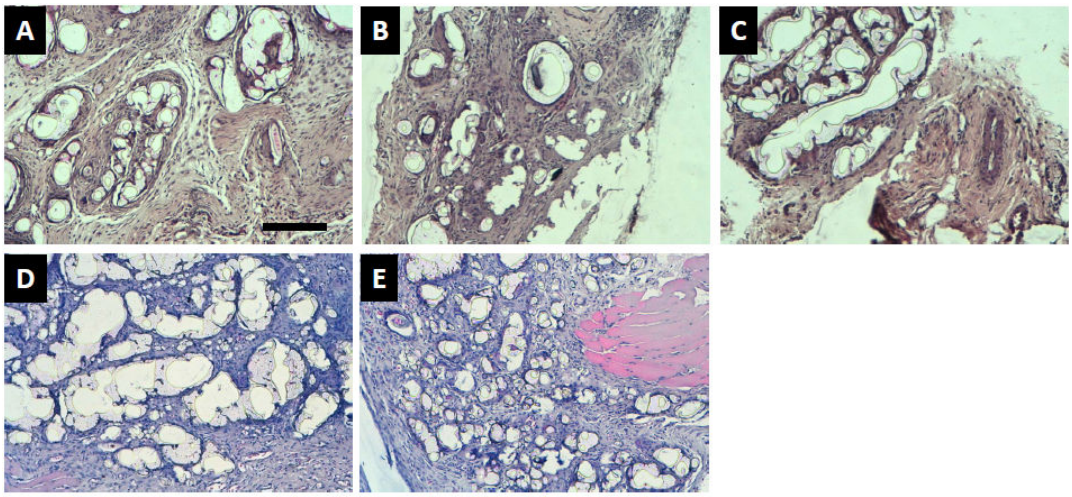

Figure 10. Histology of double-walled microspheres after 14 days implantation, x100.

Microspheres with (A) BSA-in-shell (XB) (B) simvastatin-in-core and BSA-in-shell (SB) (C) PDGF-in-shell (XP) (D) PDGF-in-core and simvastatin-in-shell (PS) (E) simvastatin-in-core and PDGF-in-shell (SP). (Scale bar represents 200 μm.)

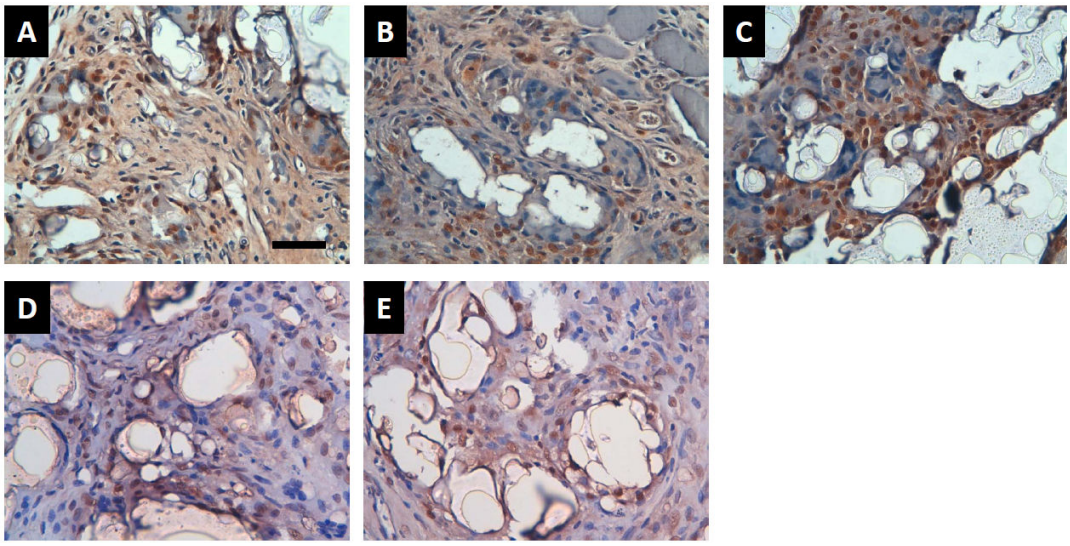

Figure 11. PCNA staining for proliferating cells at day 10, x 400.

Microspheres with (A) BSA-in-shell (XB) (B) simvastatin-in-core and BSA-in-shell (SB) (C) PDGF-in-shell (XP) (D) PDGF-in-core and simvastatin-in-shell (PS) (E) simvastatin-in-core and PDGF-in-shell (SP). Positive cells appeared in brownish color. (Scale bar represents 50μm)

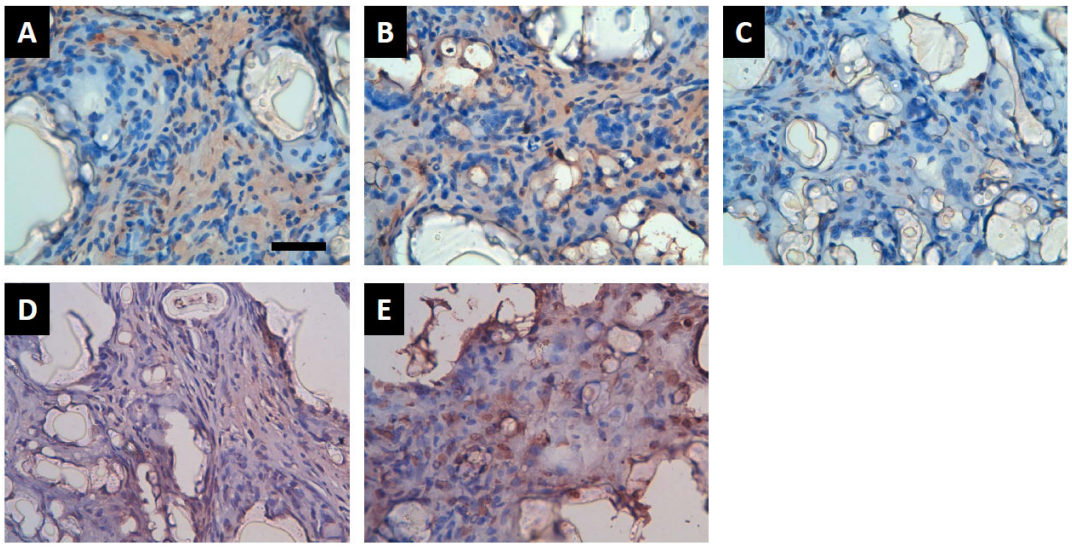

Figure 12. TUNEL staining for apoptotic cells at day 10, x 400.

Microspheres with (A) BSA-in-shell (XB) (B) simvastatin-in-core and BSA-in-shell (SB) (C) PDGF-in-shell (XP) (D) PDGF-in-core and simvastatin-in-shell (PS) (E) simvastatin-in-core and PDGF-in-shell (SP). Positive cells appeared in brownish color. (Scale bar represents 50μm)

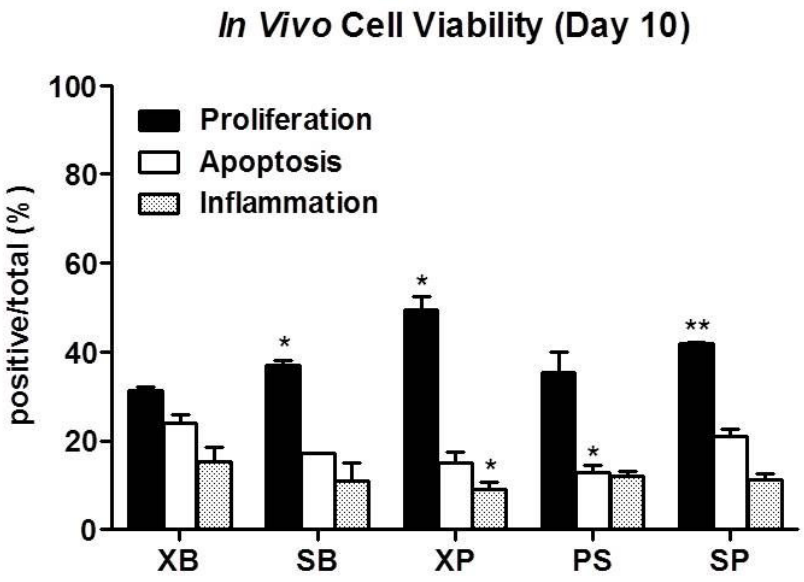

Figure 13. Quantitative data for *in vivo* cell viability after 10 days of implantation.

Each group was compared to XB (* $p<0.05$, ** $p<0.01$).

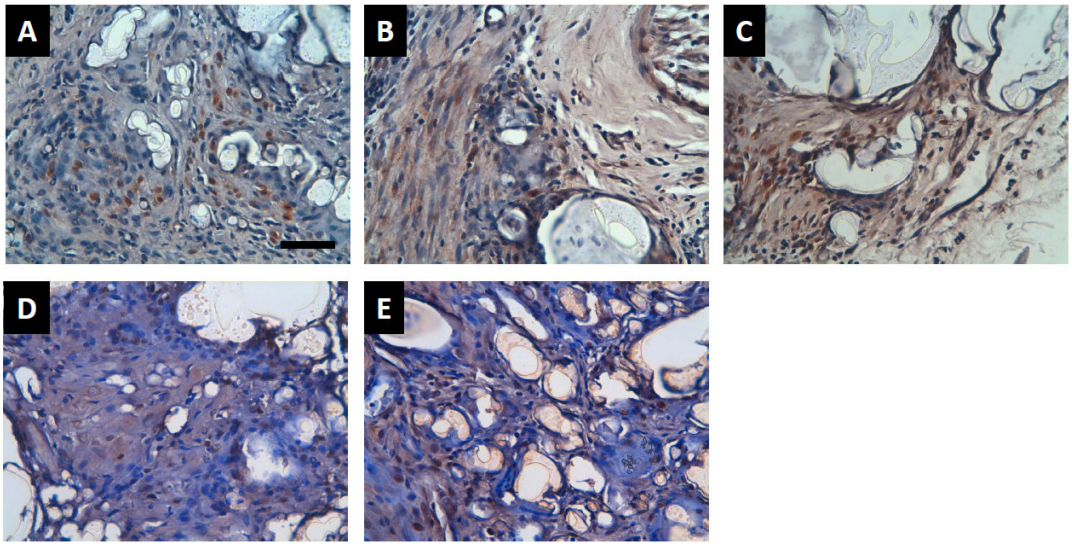

Figure 14. PCNA staining for proliferating cells at day 14, x 400.

Microspheres with (A) BSA-in-shell (XB) (B) simvastatin-in-core and BSA-in-shell (SB) (C) PDGF-in-shell (XP) (D) PDGF-in-core and simvastatin-in-shell (PS) (E) simvastatin-in-core and PDGF-in-shell (SP). Positive cells appeared in brownish color. (Scale bar represents 50μm)

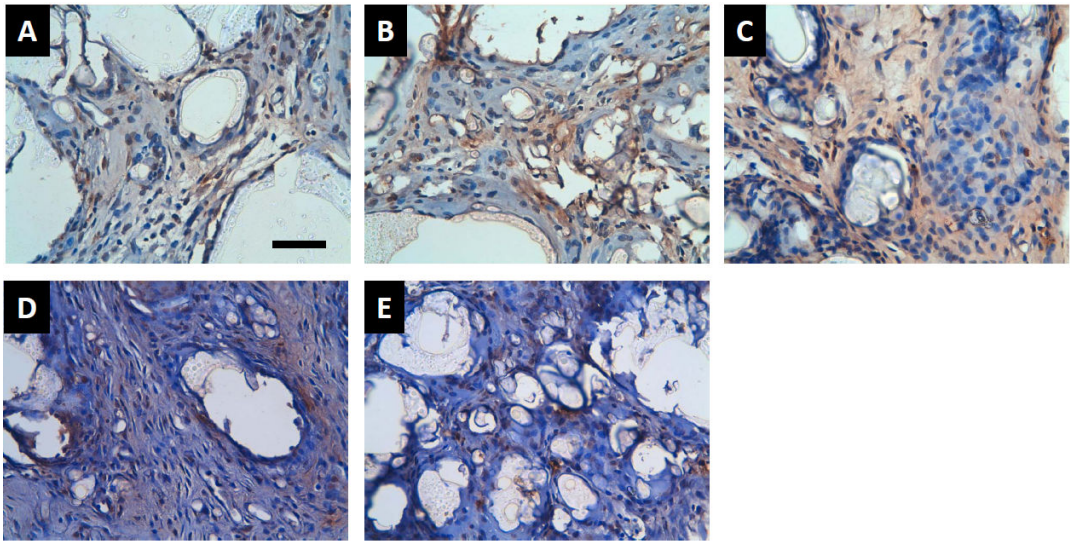

Figure 15. TUNEL staining for apoptotic cells at day 14, x 400.

Microspheres with (A) BSA-in-shell (XB) (B) simvastatin-in-core and BSA-in-shell (SB) (C) PDGF-in-shell (XP) (D) PDGF-in-core and simvastatin-in-shell (PS) (E) simvastatin-in-core and PDGF-in-shell (SP). Positive cells appeared in brownish color. (Scale bar represents 50μm)

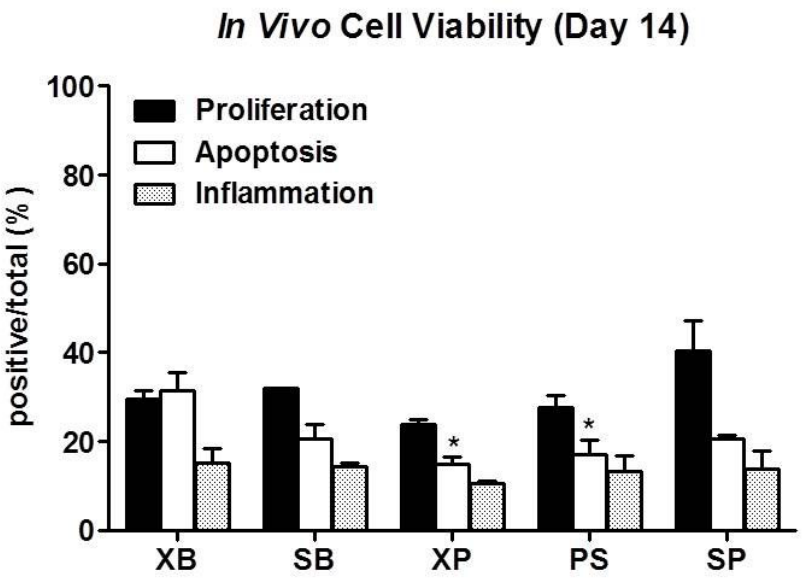

Figure 16. Quantitative data for *in vivo* cell viability after 14 days of implantation.

Each group was compared to XB (* $p<0.05$, ** $p<0.01$).

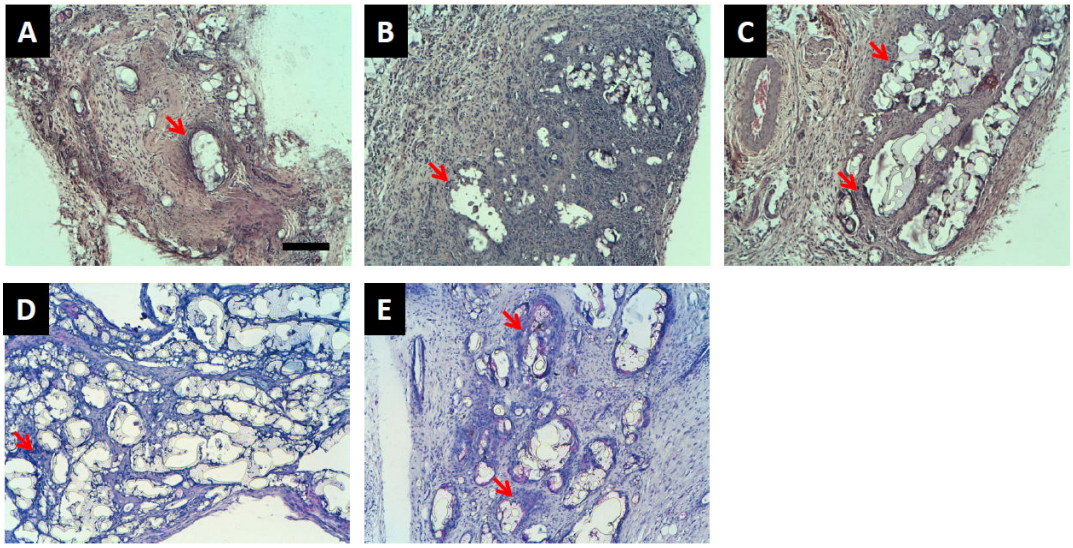

Figure 17. Fibrotic wall around the microspheres at 10 days after implantation, x 100.

Microspheres with (A) BSA-in-shell (XB) (B) simvastatin-in-core and BSA-in-shell (SB) (C) PDGF-in-shell (XP) (D) PDGF-in-core and simvastatin-in-shell (PS) (E) simvastatin-in-core and PDGF-in-shell (SP). Red-arrows indicate fibrotic wall around the microspheres. (Scale bar represents 200μm)

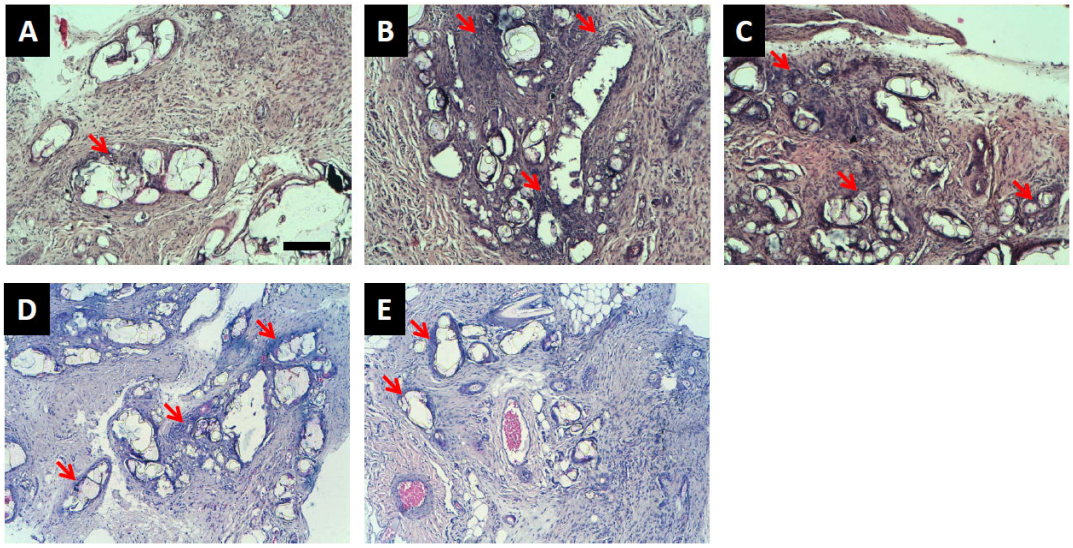

Figure 18 Fibrotic wall around the microspheres at 14 days after implantation, x 100.

Microspheres with (A) BSA-in-shell (XB) (B) simvastatin-in-core and BSA-in-shell (SB) (C) PDGF-in-shell (XP) (D) PDGF-in-core and simvastatin-in-shell (PS) (E) simvastatin-in-core and PDGF-in-shell (SP). Red-arrows indicate fibrotic wall around the microspheres. (Scale bar represents 200μm)

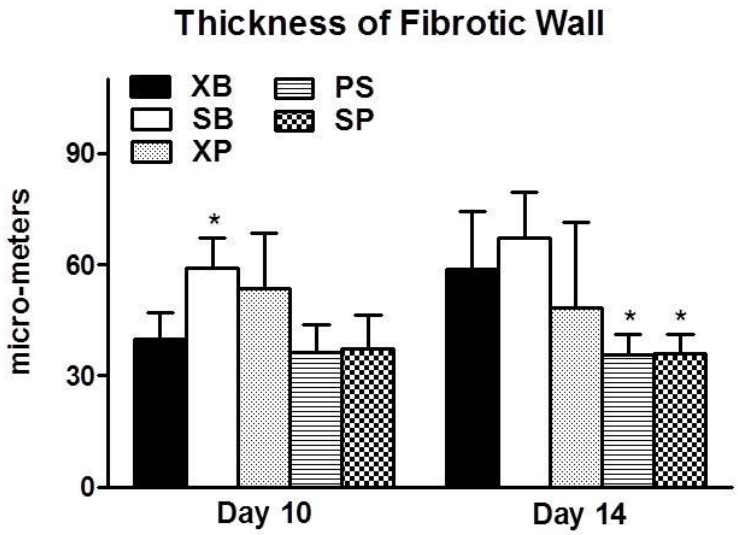

Figure 19. Quantitative data for the thickness of fibrotic wall around the microspheres after 10 and 14 days of implantation.

Each group was compared to XB (* $p<0.05$).

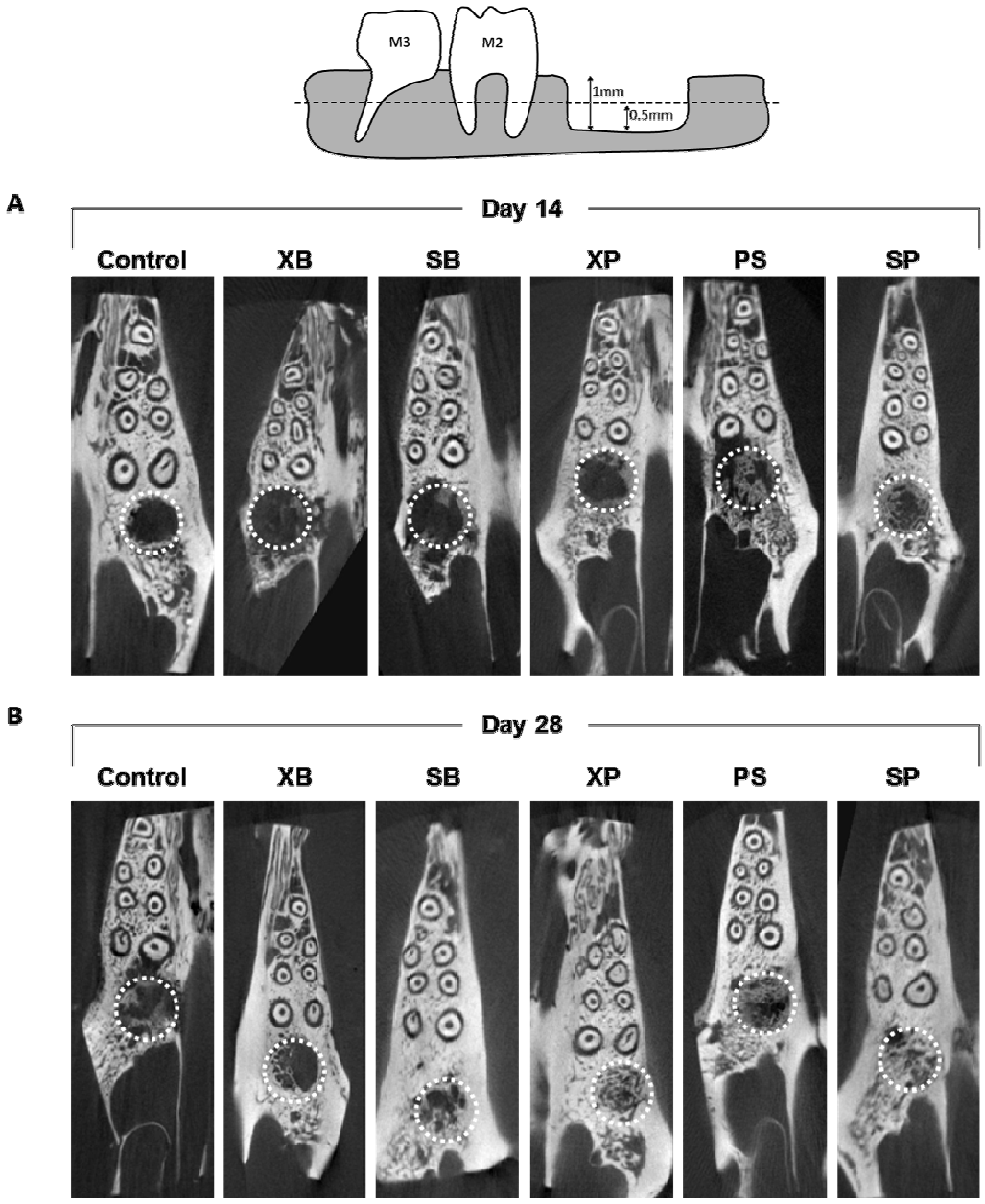

Figure 20. Transverse plan of micro-CT images in each group.

(A) 14 days and (B) 28 days after defect creation. White dashed-line indicated the region of interest.

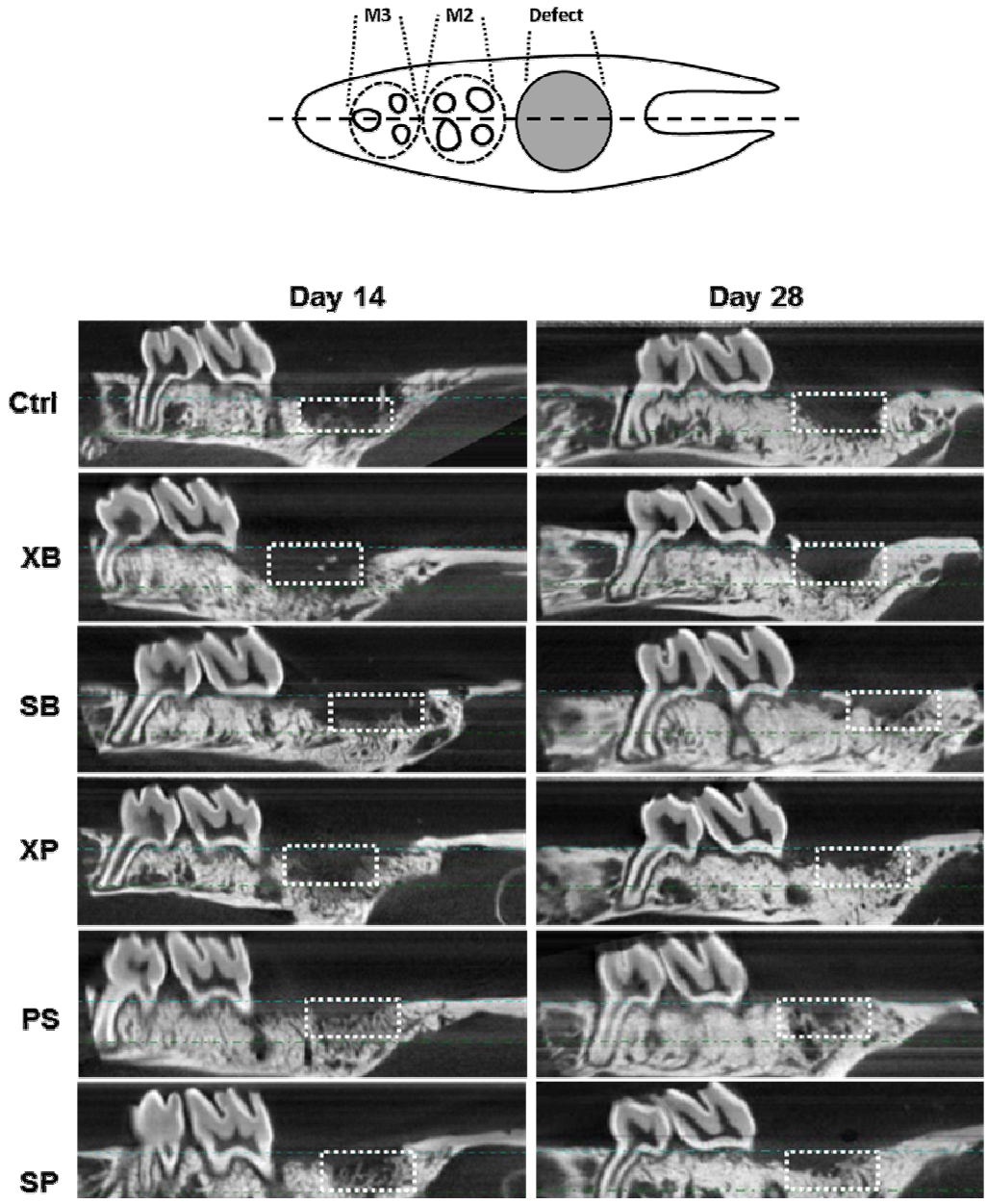

Figure 21. Saggital plan of micro-CT images in each group.

14 and 28 days after defect creation. White-dashed box represented the region of interest.

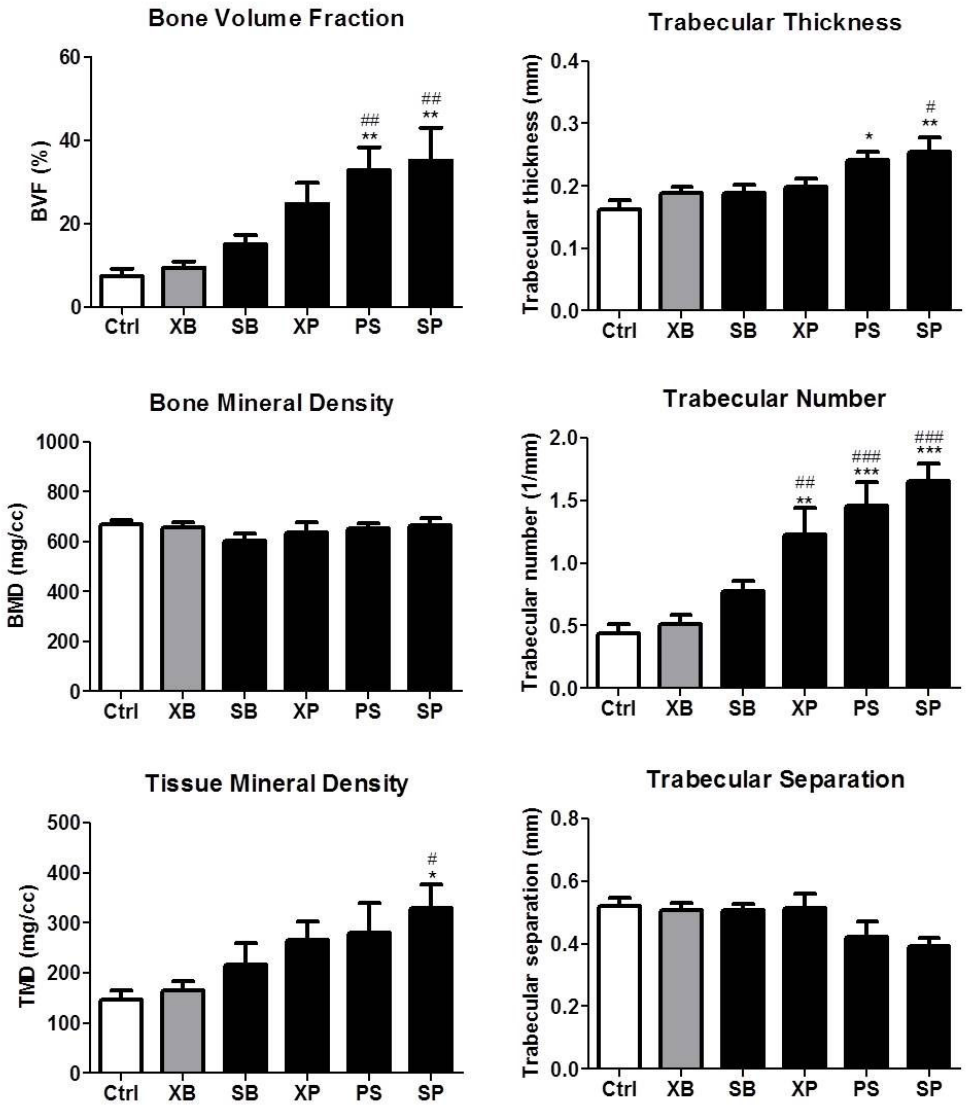

Figure 22. The micro-CT quantitative results of specimens at 14 days after surgery.

Each group was compared to XB (#) and control without any microspheres (*, Ctrl)). (*,# $p<0.05$; **,## $p<0.01$; ***,### $p<0.001$)

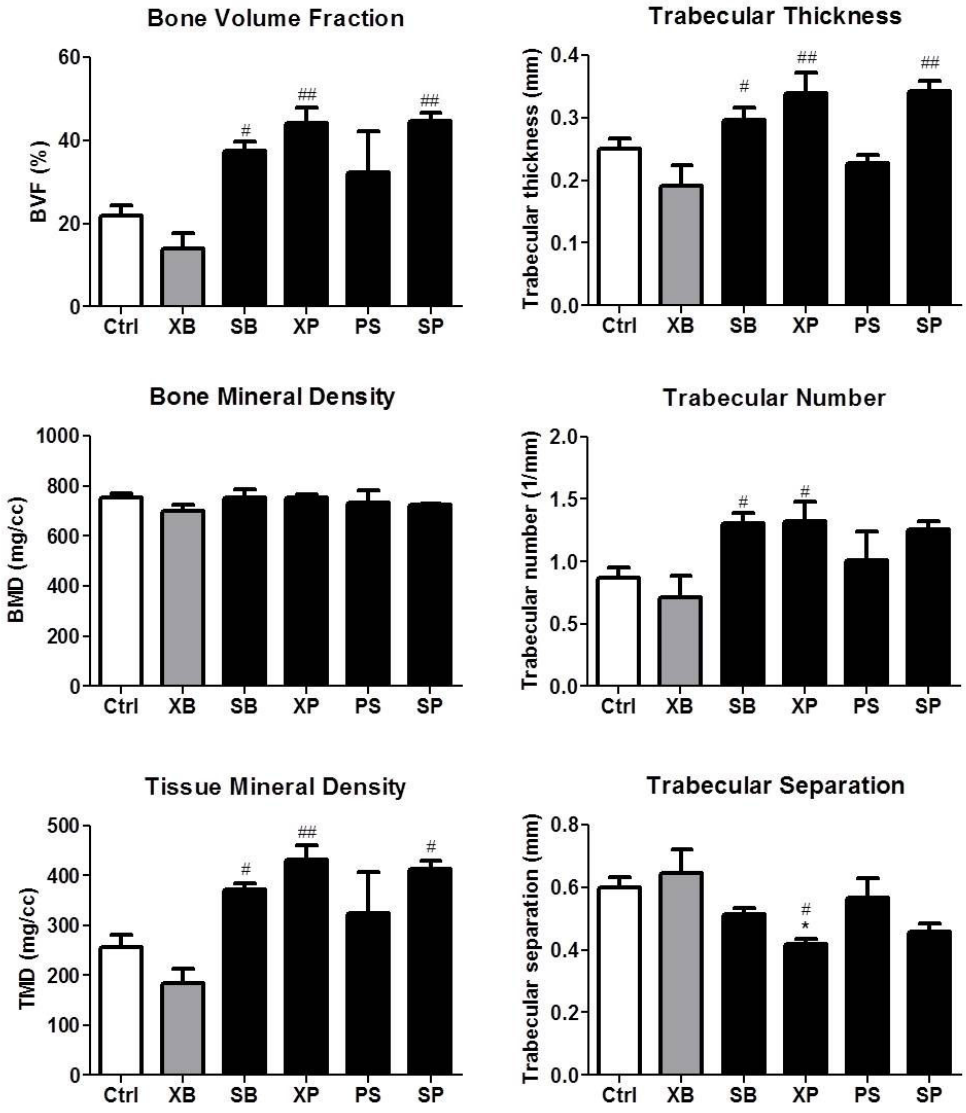

Figure 23. The micro-CT quantitative results of specimens at 28 days after surgery.

Each group was compared to XB (#) and control without any microspheres (*, Ctrl)). (*,# $p<0.05$; **,## $p<0.01$)

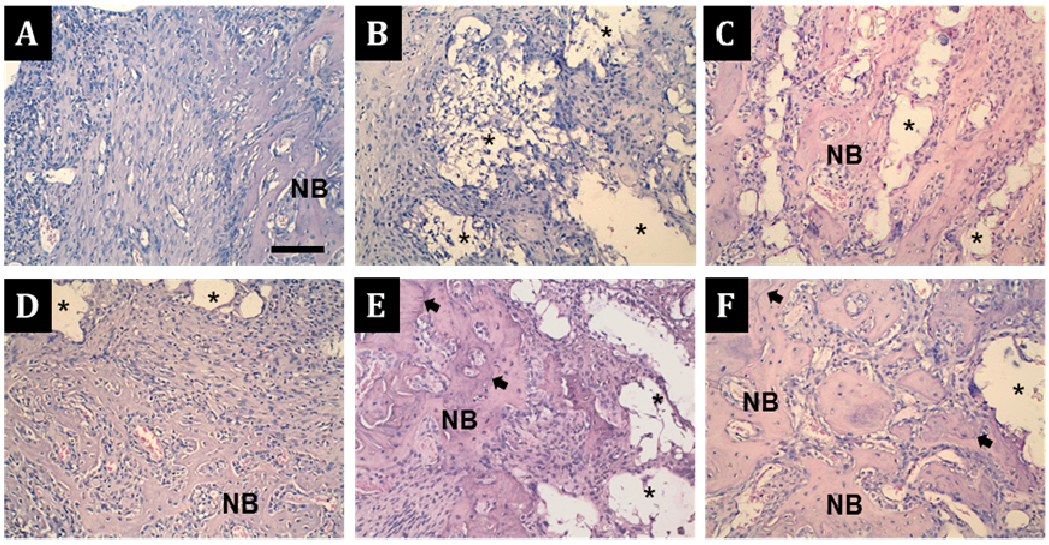

Figure 24. Descriptive histology images of each group at 14 days after implantation, x 200.

(A) Non-microspheres control and microspheres with (B) BSA-in-shell (XB) (C) simvastatin-in-core and BSA-in-shell (SB) (D) PDGF-in-shell (XP) (E) PDGF-in-core and simvastatin-in-shell (PS) (F) simvastatin-in-core and PDGF-in-shell (SP). (Scale bar represents 100μm). *Abbreviation: Asterisk: polymer residue; NB: newly-formed bone; Arrow: reversal line.*

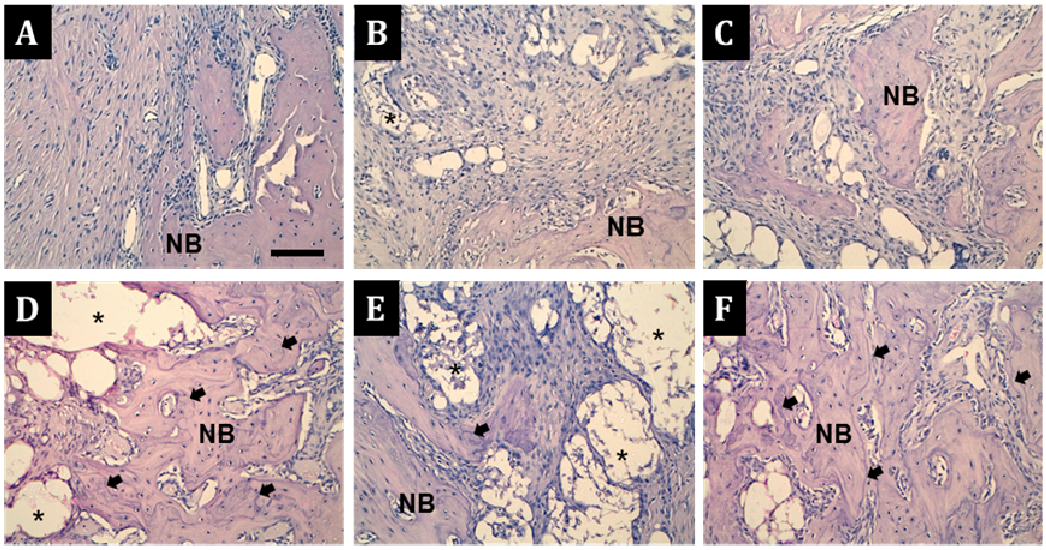

Figure 25. Descriptive histology images of each group at 28 days after implantation, x 200.

(A) Non-microspheres control and microspheres with (B) BSA-in-shell (XB) (C) simvastatin-in-core and BSA-in-shell (SB) (D) PDGF-in-shell (XP) (E) PDGF-in-core and simvastatin-in-shell (PS) (F) simvastatin-in-core and PDGF-in-shell (SP). (Scale bar represents 100μm). *Abbreviation: Asterisk: polymer residue; NB: newly-formed bone; Arrow: reversal line.*

Table 1 Summary of the fabricated double-walled microspheres of different loaded biomolecules and their encapsulation efficiencies

Sample Name	XB	SB	XP	PS	SP
Loaded Biomolecules	Core: Blank Shell: BSA	Core: Simvastatin Shell: BSA	Core: Blank Shell: PDGF	Core: PDGF Shell: Simvastatin	Core: Simvastatin Shell: PDGF
Particle size (μm)	18.1 ± 1.9	20.9 ± 1.5	18.6 ± 1.0	19.8 ± 1.3	18.8 ± 0.8
EE of core (%)	N.A.	96.2 ± 3.5	N.A.	93.8 ± 2.6	84.5 ± 2.5
EE of shell (%)	60.0 ± 2.2	63.5 ± 0.2	53.9 ± 1.1	83.2 ± 2.7	60.3 ± 2.2

EE, encapsulation efficiency; BSA, bovine serum albumin; PDGF, platelet-derived growth factor; microspheres with BSA-in-shell (XB); simvastatin-in-core and BSA-in-shell (SB); PDGF-in-shell (XP); PDGF-in-core and simvastatin-in-shell (PS); simvastatin-in-core and PDGF-in-shell (SP).

Chapter 8

BIBLIOGRAPHY

1. Williams R.C. (1990) Periodontal disease. *N Engl J Med*. 322(6):373-382.
2. Nanci A., Bosshardt D.D. (2006) Structure of periodontal tissues in health and disease. *Periodontol 2000*. 40:11-28.
3. Pihlstrom B.L., Michalowicz B.S., Johnson N.W. (2005) Periodontal diseases. *Lancet*. 366(9499):1809-1820.
4. Wolf. HF. R.K. Color Atlas of Dental Medicine: Periodontology 3rd ed: Thieme; 2005.
5. Socransky S.S. (1970) Relationship of bacteria to the etiology of periodontal disease. *J Dent Res*. 49(2):203-222.
6. Shenker B.J., Kushner M.E., Tsai C.C. (1982) Inhibition of fibroblast proliferation by Actinobacillus actinomycetemcomitans. *Infect Immun*. 38(3):986-992.
7. Shenker B.J., Tsai C.C., Taichman N.S. (1982) Suppression of lymphocyte responses by Actinobacillus actinomycetemcomitans. *J Periodontal Res*. 17(5):462-465.
8. Robertson P.B., Lantz M., Marucha P.T., Kornman K.S., Trummel C.L., Holt S.C. (1982) Collagenolytic activity associated with Bacteroides species and Actinobacillus actinomycetemcomitans. *J Periodontal Res*. 17(3):275-283.
9. Soderling E., Paunio K.U. (1981) Conditions of production and properties of the collagenolytic enzymes by two Bacillus strains from dental plaque. *J Periodontal Res*. 16(5):513-523.
10. Nair B.C., Mayberry W.R., Dziak R., Chen P.B., Levine M.J., Hausmann E. (1983) Biological effects of a purified lipopolysaccharide from Bacteroides gingivalis. *J Periodontal Res*. 18(1):40-49.
11. Raisz L.G., Nuki K., Alander C.B., Craig R.G. (1981) Interactions between bacterial endotoxin and other stimulators of bone resorption in organ culture. *J Periodontal Res*. 16(1):1-7.
12. Lindhe J., Nyman S. (1987) Clinical trials in periodontal therapy. *J Periodontal Res*. 22(3):217-221.
13. McClain P.K., Schallhorn R.G. (2000) Focus on furcation defects--guided tissue regeneration in combination with bone grafting. *Periodontol 2000*. 22:190-212.
14. Hammerle C.H., Jung R.E. (2003) Bone augmentation by means of barrier membranes. *Periodontol 2000*. 33:36-53.
15. Aichelmann-Reidy M.E., Reynolds M.A. (2008) Predictability of clinical outcomes following regenerative therapy in intrabony defects. *J Periodontol*. 79(3):387-393.

16. Zeichner-David M. (2006) Regeneration of periodontal tissues: cementogenesis revisited. *Periodontol 2000*. 41:196-217.
17. Grzesik W.J., Narayanan A.S. (2002) Cementum and periodontal wound healing and regeneration. *Crit Rev Oral Biol Med*. 13(6):474-484.
18. Elangovan S., Srinivasan S., Ayilavarapu S. (2009) Novel regenerative strategies to enhance periodontal therapy outcome. *Expert Opin Biol Ther*. 9(4):399-410.
19. Douglass G.L. (2005) Periodontics--tissue engineering and the future. *J Calif Dent Assoc*. 33(3):203-204.
20. Bartold P.M., McCulloch C.A., Narayanan A.S., Pitaru S. (2000) Tissue engineering: a new paradigm for periodontal regeneration based on molecular and cell biology. *Periodontol 2000*. 24:253-269.
21. Kao R.T., Conte G., Nishimine D., Dault S. (2005) Tissue engineering for periodontal regeneration. *J Calif Dent Assoc*. 33(3):205-215.
22. Lumelsky N.L. (2007) Commentary: engineering of tissue healing and regeneration. *Tissue Eng*. 13(7):1393-1398.
23. Taba M., Jr., Jin Q., Sugai J.V., Giannobile W.V. (2005) Current concepts in periodontal bioengineering. *Orthod Craniofac Res*. 8(4):292-302.
24. Chen F.M., Ma Z.W., Wang Q.T., Wu Z.F. (2009) Gene delivery for periodontal tissue engineering: current knowledge - future possibilities. *Curr Gene Ther*. 9(4):248-266.
25. Chen F.M., Shelton R.M., Jin Y., Chapple I.L. (2009) Localized delivery of growth factors for periodontal tissue regeneration: role, strategies, and perspectives. *Med Res Rev*. 29(3):472-513.
26. Kaigler D., Cirelli J.A., Giannobile W.V. (2006) Growth factor delivery for oral and periodontal tissue engineering. *Expert Opin Drug Deliv*. 3(5):647-662.
27. Aukhil I. (2000) Biology of wound healing. *Periodontol 2000*. 22:44-50.
28. Stadelmann W.K., Digenis A.G., Tobin G.R. (1998) Physiology and healing dynamics of chronic cutaneous wounds. *Am J Surg*. 176(2A Suppl):26S-38S.
29. Midwood K.S., Williams L.V., Schwarzbauer J.E. (2004) Tissue repair and the dynamics of the extracellular matrix. *Int J Biochem Cell Biol*. 36(6):1031-1037.
30. Polimeni G., Xiropaidis A.V., Wikesjo U.M. (2006) Biology and principles of periodontal wound healing/regeneration. *Periodontol 2000*. 41:30-47.
31. Greenhalgh D.G. (1998) The role of apoptosis in wound healing. *Int J Biochem Cell Biol*. 30(9):1019-1030.
32. DiPietro L.A. (1995) Wound healing: the role of the macrophage and other immune cells. *Shock*. 4(4):233-240.
33. Romo T., Pearson J.M. Wound Healing, Skin2005 December 27, 2006.
34. Martin P. (1997) Wound healing--aiming for perfect skin regeneration. *Science*.

276(5309):75-81.

35. Wikesjo U.M., Selvig K.A. (1999) Periodontal wound healing and regeneration. *Periodontol 2000*. 19:21-39.
36. Selvig K.A., Bogle G., Claffey N.M. (1988) Collagen linkage in periodontal connective tissue reattachment. An ultrastructural study in beagle dogs. *J Periodontol*. 59(11):758-768.
37. Selvig K.A., Sigurdsson T.J., Wikesjo U.M. (1995) "Collagen adhesion" revisited. *Int J Periodontics Restorative Dent*. 15(6):528-537.
38. Cardaropoli G., Araujo M., Lindhe J. (2003) Dynamics of bone tissue formation in tooth extraction sites. An experimental study in dogs. *J Clin Periodontol*. 30(9):809-818.
39. Hill P.A. (1998) Bone remodelling. *Br J Orthod*. 25(2):101-107.
40. Giannobile W.V. (1996) Periodontal tissue engineering by growth factors. *Bone*. 19(1 Suppl):23S-37S.
41. Graves D.T., Cochran D.L. (1990) Mesenchymal cell growth factors. *Crit Rev Oral Biol Med*. 1(1):17-36.
42. Mohan S., Baylink D.J. (1991) Bone growth factors. *Clin Orthop Relat Res*. (263):30-48.
43. Chen F.M., Jin Y. (2010) Periodontal tissue engineering and regeneration: current approaches and expanding opportunities. *Tissue Eng Part B Rev*. 16(2):219-255.
44. Ramseier C.A., Rasperini G., Batia S., Giannobile W.V. (2012) Advanced reconstructive technologies for periodontal tissue repair. *Periodontol 2000*. 59(1):185-202.
45. Caffesse R.G., Becker W. (1991) Principles and techniques of guided tissue regeneration. *Dent Clin North Am*. 35(3):479-494.
46. Clem D.S., 3rd, Bishop J.P. (1991) Guided tissue regeneration in periodontal therapy. *J Calif Dent Assoc*. 19(12):67-73.
47. Midda M., Rees J.S. (1990) Guided tissue regeneration: an overview. *J R Coll Surg Edinb*. 35(5):275-278.
48. Murphy K.G., Gunsolley J.C. (2003) Guided tissue regeneration for the treatment of periodontal intrabony and furcation defects. A systematic review. *Ann Periodontol*. 8(1):266-302.
49. Cortellini P., Bowers G.M. (1995) Periodontal regeneration of intrabony defects: an evidence-based treatment approach. *Int J Periodontics Restorative Dent*. 15(2):128-145.
50. Karring T., Cortellini P. (1999) Regenerative therapy: furcation defects. *Periodontol 2000*. 19:115-137.
51. Machtei E.E., Schallhorn R.G. (1995) Successful regeneration of mandibular

Class II furcation defects: an evidence-based treatment approach. *Int J Periodontics Restorative Dent*. 15(2):146-167.

52. Pini Prato G., Clauser C., Cortellini P., Tinti C., Vincenzi G., Pagliaro U. (1996) Guided tissue regeneration versus mucogingival surgery in the treatment of human buccal recessions. A 4-year follow-up study. *J Periodontol*. 67(11):1216-1223.
53. Hanes P.J. (2007) Bone replacement grafts for the treatment of periodontal intrabony defects. *Oral Maxillofac Surg Clin North Am*. 19(4):499-512, vi.
54. Hallman M., Thor A. (2008) Bone substitutes and growth factors as an alternative/complement to autogenous bone for grafting in implant dentistry. *Periodontol 2000*. 47:172-192.
55. Khan S.N., Cammisa F.P., Jr., Sandhu H.S., Diwan A.D., Girardi F.P., Lane J.M. (2005) The biology of bone grafting. *J Am Acad Orthop Surg*. 13(1):77-86.
56. Kao R.T., Murakami S., Beirne O.R. (2009) The use of biologic mediators and tissue engineering in dentistry. *Periodontol 2000*. 50:127-153.
57. Kaigler D., Avila G., Wisner-Lynch L., Nevins M.L., Nevins M., Rasperini G., Lynch S.E., Giannobile W.V. (2011) Platelet-derived growth factor applications in periodontal and peri-implant bone regeneration. *Expert Opin Biol Ther*. 11(3):375-385.
58. Javed F., Al-Askar M., Al-Rasheed A., Al-Hezaimi K. (2011) Significance of the platelet-derived growth factor in periodontal tissue regeneration. *Arch Oral Biol*. 56(12):1476-1484.
59. Howell T.H., Fiorellini J.P., Paquette D.W., Offenbacher S., Giannobile W.V., Lynch S.E. (1997) A phase I/II clinical trial to evaluate a combination of recombinant human platelet-derived growth factor-BB and recombinant human insulin-like growth factor-I in patients with periodontal disease. *J Periodontol*. 68(12):1186-1193.
60. Nevins M., Hanratty J., Lynch S.E. (2007) Clinical results using recombinant human platelet-derived growth factor and mineralized freeze-dried bone allograft in periodontal defects. *Int J Periodontics Restorative Dent*. 27(5):421-427.
61. Nevins M., Giannobile W.V., McGuire M.K., Kao R.T., Mellonig J.T., Hinrichs J.E., McAllister B.S., Murphy K.S., McClain P.K., Nevins M.L., Paquette D.W., Han T.J., Reddy M.S., Lavin P.T., Genco R.J., Lynch S.E. (2005) Platelet-derived growth factor stimulates bone fill and rate of attachment level gain: results of a large multicenter randomized controlled trial. *J Periodontol*. 76(12):2205-2215.
62. McAllister B.S., Haghighat K., Prasad H.S., Rohrer M.D. (2010) Histologic evaluation of recombinant human platelet-derived growth factor-BB after use in extraction socket defects: a case series. *Int J Periodontics Restorative Dent*.

30(4):365-373.

63. Jayakumar A., Rajababu P., Rohini S., Butchibabu K., Naveen A., Reddy P.K., Vidyasagar S., Satyanarayana D., Pavan Kumar S. (2011) Multi-centre, randomized clinical trial on the efficacy and safety of recombinant human platelet-derived growth factor with beta-tricalcium phosphate in human intra-osseous periodontal defects. *J Clin Periodontol*. 38(2):163-172.
64. Park Y.J., Lee Y.M., Lee J.Y., Seol Y.J., Chung C.P., Lee S.J. (2000) Controlled release of platelet-derived growth factor-BB from chondroitin sulfate-chitosan sponge for guided bone regeneration. *J Control Release*. 67(2-3):385-394.
65. Lin Z., Sugai J.V., Jin Q., Chandler L.A., Giannobile W.V. (2008) Platelet-derived growth factor-B gene delivery sustains gingival fibroblast signal transduction. *J Periodontal Res*. 43(4):440-449.
66. Lynch S.E., Williams R.C., Polson A.M., Howell T.H., Reddy M.S., Zappa U.E., Antoniades H.N. (1989) A combination of platelet-derived and insulin-like growth factors enhances periodontal regeneration. *J Clin Periodontol*. 16(8):545-548.
67. Urban I., Caplanis N., Lozada J.L. (2009) Simultaneous vertical guided bone regeneration and guided tissue regeneration in the posterior maxilla using recombinant human platelet-derived growth factor: a case report. *J Oral Implantol*. 35(5):251-256.
68. Schwarz F., Ferrari D., Podolsky L., Mihatovic I., Becker J. (2010) Initial pattern of angiogenesis and bone formation following lateral ridge augmentation using rhPDGF and guided bone regeneration: an immunohistochemical study in dogs. *Clin Oral Implants Res*. 21(1):90-99.
69. Schwarz F., Sager M., Ferrari D., Mihatovic I., Becker J. (2009) Influence of recombinant human platelet-derived growth factor on lateral ridge augmentation using biphasic calcium phosphate and guided bone regeneration: a histomorphometric study in dogs. *J Periodontol*. 80(8):1315-1323.
70. Simion M., Rocchietta I., Kim D., Nevins M., Fiorellini J. (2006) Vertical ridge augmentation by means of deproteinized bovine bone block and recombinant human platelet-derived growth factor-BB: a histologic study in a dog model. *Int J Periodontics Restorative Dent*. 26(5):415-423.
71. Lioubavina-Hack N., Carmagnola D., Lynch S.E., Karring T. (2005) Effect of Bio-Oss with or without platelet-derived growth factor on bone formation by "guided tissue regeneration": a pilot study in rats. *J Clin Periodontol*. 32(12):1254-1260.
72. Park J.B., Matsuura M., Han K.Y., Norderyd O., Lin W.L., Genco R.J., Cho M.I. (1995) Periodontal regeneration in class III furcation defects of beagle dogs using

guided tissue regenerative therapy with platelet-derived growth factor. *J Periodontol*. 66(6):462-477.

73. Todd P.A., Goa K.L. (1990) Simvastatin. A review of its pharmacological properties and therapeutic potential in hypercholesterolaemia. *Drugs*. 40(4):583-607.
74. Hunninghake D.B. (1998) Therapeutic efficacy of the lipid-lowering armamentarium: the clinical benefits of aggressive lipid-lowering therapy. *Am J Med*. 104(2A):9S-13S.
75. Mundy G., Garrett R., Harris S., Chan J., Chen D., Rossini G., Boyce B., Zhao M., Gutierrez G. (1999) Stimulation of bone formation in vitro and in rodents by statins. *Science*. 286(5446):1946-1949.
76. Garrett I.R., Gutierrez G., Mundy G.R. (2001) Statins and bone formation. *Curr Pharm Des*. 7(8):715-736.
77. Thylin M.R., McConnell J.C., Schmid M.J., Reckling R.R., Ojha J., Bhattacharyya I., Marx D.B., Reinhardt R.A. (2002) Effects of simvastatin gels on murine calvarial bone. *J Periodontol*. 73(10):1141-1148.
78. Stein D., Lee Y., Schmid M.J., Killpack B., Genrich M.A., Narayana N., Marx D.B., Cullen D.M., Reinhardt R.A. (2005) Local simvastatin effects on mandibular bone growth and inflammation. *J Periodontol*. 76(11):1861-1870.
79. Bradley J.D., Cleverly D.G., Burns A.M., Helm N.B., Schmid M.J., Marx D.B., Cullen D.M., Reinhardt R.A. (2007) Cyclooxygenase-2 inhibitor reduces simvastatin-induced bone morphogenetic protein-2 and bone formation in vivo. *J Periodontal Res*. 42(3):267-273.
80. Jadhav S.B., Jain G.K. (2006) Statins and osteoporosis: new role for old drugs. *J Pharm Pharmacol*. 58(1):3-18.
81. Yamashita M., Otsuka F., Mukai T., Otani H., Inagaki K., Miyoshi T., Goto J., Yamamura M., Makino H. (2008) Simvastatin antagonizes tumor necrosis factor-alpha inhibition of bone morphogenetic proteins-2-induced osteoblast differentiation by regulating Smad signaling and Ras/Rho-mitogen-activated protein kinase pathway. *J Endocrinol*. 196(3):601-613.
82. Chen P.Y., Sun J.S., Tsuang Y.H., Chen M.H., Weng P.W., Lin F.H. (2010) Simvastatin promotes osteoblast viability and differentiation via Ras/Smad/Erk/BMP-2 signaling pathway. *Nutr Res*. 30(3):191-199.
83. Kim I.S., Jeong B.C., Kim O.S., Kim Y.J., Lee S.E., Lee K.N., Koh J.T., Chung H.J. (2011) Lactone form 3-hydroxy-3-methylglutaryl-coenzyme A reductase inhibitors (statins) stimulate the osteoblastic differentiation of mouse periodontal ligament cells via the ERK pathway. *J Periodontal Res*. 46(2):204-213.
84. Montagnani A., Gonnelli S., Cepollaro C., Pacini S., Campagna M.S., Franci

M.B., Lucani B., Gennari C. (2003) Effect of simvastatin treatment on bone mineral density and bone turnover in hypercholesterolemic postmenopausal women: a 1-year longitudinal study. *Bone*. 32(4):427-433.

85. Nyan M., Sato D., Oda M., Machida T., Kobayashi H., Nakamura T., Kasugai S. (2007) Bone formation with the combination of simvastatin and calcium sulfate in critical-sized rat calvarial defect. *J Pharmacol Sci*. 104(4):384-386.
86. Seto H., Ohba H., Tokunaga K., Hama H., Horibe M., Nagata T. (2008) Topical administration of simvastatin recovers alveolar bone loss in rats. *J Periodontal Res*. 43(3):261-267.
87. Vaziri H., Naserhojjati-Roodsari R., Tahsili-Fahadan N., Khojasteh A., Mashhadi-Abbas F., Eslami B., Dehpour A.R. (2007) Effect of simvastatin administration on periodontitis-associated bone loss in ovariectomized rats. *J Periodontol*. 78(8):1561-1567.
88. Nassar P.O., Nassar C.A., Guimaraes M.R., Aquino S.G., Andia D.C., Muscara M.N., Spolidorio D.M., Rossa C., Jr., Spolidorio L.C. (2009) Simvastatin therapy in cyclosporine A-induced alveolar bone loss in rats. *J Periodontal Res*. 44(4):479-488.
89. Park J.B. (2009) The use of simvastatin in bone regeneration. *Med Oral Patol Oral Cir Bucal*. 14(9):e485-488.
90. Pradeep A.R., Thorat M.S. (2010) Clinical effect of subgingivally delivered simvastatin in the treatment of patients with chronic periodontitis: a randomized clinical trial. *J Periodontol*. 81(2):214-222.
91. Chen R.R., Silva E.A., Yuen W.W., Brock A.A., Fischbach C., Lin A.S., Guldberg R.E., Mooney D.J. (2007) Integrated approach to designing growth factor delivery systems. *Faseb J*. 21(14):3896-3903.
92. King G.N. (2001) The importance of drug delivery to optimize the effects of bone morphogenetic proteins during periodontal regeneration. *Curr Pharm Biotechnol*. 2(2):131-142.
93. Rutherford R.B., Ryan M.E., Kennedy J.E., Tucker M.M., Charette M.F. (1993) Platelet-derived growth factor and dexamethasone combined with a collagen matrix induce regeneration of the periodontium in monkeys. *J Clin Periodontol*. 20(7):537-544.
94. Blumenthal N.M., Koh-Kunst G., Alves M.E., Miranda D., Sorensen R.G., Wozney J.M., Wikesjo U.M. (2002) Effect of surgical implantation of recombinant human bone morphogenetic protein-2 in a bioabsorbable collagen sponge or calcium phosphate putty carrier in intrabony periodontal defects in the baboon. *J Periodontol*. 73(12):1494-1506.
95. Nakahara T., Nakamura T., Kobayashi E., Inoue M., Shigeno K., Tabata Y., Eto

K., Shimizu Y. (2003) Novel approach to regeneration of periodontal tissues based on in situ tissue engineering: effects of controlled release of basic fibroblast growth factor from a sandwich membrane. *Tissue Eng*. 9(1):153-162.

96. Sato Y., Kikuchi M., Ohata N., Tamura M., Kuboki Y. (2004) Enhanced cementum formation in experimentally induced cementum defects of the root surface with the application of recombinant basic fibroblast growth factor in collagen gel in vivo. *J Periodontol*. 75(2):243-248.
97. Ahmed T.A., Dare E.V., Hincke M. (2008) Fibrin: a versatile scaffold for tissue engineering applications. *Tissue Eng Part B Rev*. 14(2):199-215.
98. Hall H. (2007) Modified fibrin hydrogel matrices: both, 3D-scaffolds and local and controlled release systems to stimulate angiogenesis. *Curr Pharm Des*. 13(35):3597-3607.
99. Tessmar J.K., Gopferich A.M. (2007) Matrices and scaffolds for protein delivery in tissue engineering. *Adv Drug Deliv Rev*. 59(4-5):274-291.
100. Yang Y., El Haj A.J. (2006) Biodegradable scaffolds--delivery systems for cell therapies. *Expert Opin Biol Ther*. 6(5):485-498.
101. Cartmell S. (2009) Controlled release scaffolds for bone tissue engineering. *J Pharm Sci*. 98(2):430-441.
102. Griffith L.G., Naughton G. (2002) Tissue engineering--current challenges and expanding opportunities. *Science*. 295(5557):1009-1014.
103. Drury J.L., Mooney D.J. (2003) Hydrogels for tissue engineering: scaffold design variables and applications. *Biomaterials*. 24(24):4337-4351.
104. (!!! INVALID CITATION !!!).
105. Varkey M., Gittens S.A., Uludag H. (2004) Growth factor delivery for bone tissue repair: an update. *Expert Opin Drug Deliv*. 1(1):19-36.
106. Kobsa S., Saltzman W.M. (2008) Bioengineering approaches to controlled protein delivery. *Pediatr Res*. 63(5):513-519.
107. Andreadis S.T., Geer D.J. (2006) Biomimetic approaches to protein and gene delivery for tissue regeneration. *Trends Biotechnol*. 24(7):331-337.
108. Vasita R., Katti D.S. (2006) Growth factor-delivery systems for tissue engineering: a materials perspective. *Expert Rev Med Devices*. 3(1):29-47.
109. Balasubramanian V., Onaca O., Enea R., Hughes D.W., Palivan C.G. (2010) Protein delivery: from conventional drug delivery carriers to polymeric nanoreactors. *Expert Opin Drug Deliv*. 7(1):63-78.
110. Guldberg R.E. (2009) Spatiotemporal delivery strategies for promoting musculoskeletal tissue regeneration. *J Bone Miner Res*. 24(9):1507-1511.
111. Langer R. (1998) Drug delivery and targeting. *Nature*. 392(6679 Suppl):5-10.
112. Tabata Y. (2006) Regenerative inductive therapy based on DDS technology of

protein and gene. *J Drug Target*. 14(7):483-495.

113. Chen F.M., Zhang M., Wu Z.F. (2010) Toward delivery of multiple growth factors in tissue engineering. *Biomaterials*. 31(24):6279-6308.
114. Bourque W.T., Gross M., Hall B.K. (1993) Expression of four growth factors during fracture repair. *Int J Dev Biol*. 37(4):573-579.
115. Bostrom M.P., Lane J.M., Berberian W.S., Missri A.A., Tomin E., Weiland A., Doty S.B., Glaser D., Rosen V.M. (1995) Immunolocalization and expression of bone morphogenetic proteins 2 and 4 in fracture healing. *J Orthop Res*. 13(3):357-367.
116. Yu Y., Yang J.L., Chapman-Sheath P.J., Walsh W.R. (2002) TGF-beta, BMPS, and their signal transducing mediators, Smads, in rat fracture healing. *J Biomed Mater Res*. 60(3):392-397.
117. Simmons C.A., Alsberg E., Hsiong S., Kim W.J., Mooney D.J. (2004) Dual growth factor delivery and controlled scaffold degradation enhance in vivo bone formation by transplanted bone marrow stromal cells. *Bone*. 35(2):562-569.
118. Tayalia P., Mooney D.J. (2009) Controlled growth factor delivery for tissue engineering. *Adv Mater*. 21(32-33):3269-3285.
119. Biondi M., Ungaro F., Quaglia F., Netti P.A. (2008) Controlled drug delivery in tissue engineering. *Adv Drug Deliv Rev*. 60(2):229-242.
120. Richardson T.P., Peters M.C., Ennett A.B., Mooney D.J. (2001) Polymeric system for dual growth factor delivery. *Nat Biotechnol*. 19(11):1029-1034.
121. Chang P.C., Chung M.C., Lei C., Chong L.Y., Wang C.H. (2012) Biocompatibility of PDGF-simvastatin double-walled PLGA (PDLLA) microspheres for dentoalveolar regeneration: A preliminary study. *J Biomed Mater Res A*.
122. Nie H., Dong Z., Arifin D.Y., Hu Y., Wang C.H. (2010) Core/shell microspheres via coaxial electrohydrodynamic atomization for sequential and parallel release of drugs. *J Biomed Mater Res A*. 95(3):709-716.
123. Naraharisetti P.K., Guan Lee H.C., Fu Y.C., Lee D.J., Wang C.H. (2006) In vitro and in vivo release of gentamicin from biodegradable discs. *J Biomed Mater Res B Appl Biomater*. 77(2):329-337.
124. Shive M.S., Anderson J.M. (1997) Biodegradation and biocompatibility of PLA and PLGA microspheres. *Adv Drug Deliv Rev*. 28(1):5-24.
125. Miller R.A., Brady J.M., Cutright D.E. (1977) Degradation rates of oral resorbable implants (polylactates and polyglycolates): rate modification with changes in PLA/PGA copolymer ratios. *J Biomed Mater Res*. 11(5):711-719.
126. Nie H., Dong Z., Arifin D.Y., Hu Y., Wang C.H. Core/shell microspheres via coaxial electrohydrodynamic atomization for sequential and parallel release of

drugs. *J Biomed Mater Res A*. 95(3):709-716.

127. Williams D.F. (2008) On the mechanisms of biocompatibility. *Biomaterials*. 29(20):2941-2953.
128. Yoon S.J., Kim S.H., Ha H.J., Ko Y.K., So J.W., Kim M.S., Yang Y.I., Khang G., Rhee J.M., Lee H.B. (2008) Reduction of inflammatory reaction of poly(d,l-lactic-co-glycolic Acid) using demineralized bone particles. *Tissue Eng Part A*. 14(4):539-547.
129. Pariente J.L., Kim B.S., Atala A. (2001) In vitro biocompatibility assessment of naturally derived and synthetic biomaterials using normal human urothelial cells. *J Biomed Mater Res*. 55(1):33-39.
130. Qu X.H., Wu Q., Zhang K.Y., Chen G.Q. (2006) In vivo studies of poly(3-hydroxybutyrate-co-3-hydroxyhexanoate) based polymers: biodegradation and tissue reactions. *Biomaterials*. 27(19):3540-3548.
131. Ntaios G., Savopoulos C., Karamitsos D., Economou I., Destanis E., Chryssogonidis I., Pidonia I., Zebekakis P., Polatides C., Sion M., Grekas D., Hatzitolios A. (2010) The effect of folic acid supplementation on carotid intima-media thickness in patients with cardiovascular risk: a randomized, placebo-controlled trial. *Int J Cardiol*. 143(1):16-19.
132. Bracht L., Caparroz-Assef S.M., Magon T.F., Ritter A.M., Cuman R.K., Bersani-Amado C.A. (2011) Topical anti-inflammatory effect of hypocholesterolaemic drugs. *J Pharm Pharmacol*. 63(7):971-975.
133. Pagkalos J., Cha J.M., Kang Y., Heliotis M., Tsiridis E., Mantalaris A. (2010) Simvastatin induces osteogenic differentiation of murine embryonic stem cells. *J Bone Miner Res*. 25(11):2470-2478.
134. Jeon J.H., Piepgrass W.T., Lin Y.L., Thomas M.V., Puleo D.A. (2008) Localized intermittent delivery of simvastatin hydroxyacid stimulates bone formation in rats. *J Periodontol*. 79(8):1457-1464.
135. Lee Y., Schmid M.J., Marx D.B., Beatty M.W., Cullen D.M., Collins M.E., Reinhardt R.A. (2008) The effect of local simvastatin delivery strategies on mandibular bone formation in vivo. *Biomaterials*. 29(12):1940-1949.
136. Joles J., Willekes-Koolschijn N., Koomans H., Van Tol A., Geelhoed-Mieras T., Crommelin D., Van Bloois L., Krajnc-Franken M., Cohen L., Griffioen M., et al. (1992) Subcutaneous administration of HMG-CoA reductase inhibitors in hyperlipidaemic and normal rats. *Lab Anim*. 26(4):269-280.
137. Sugiyama T., Nakagawa T., Sato C., Fujii T., Mine K., Shimizu K., Murata T., Tagawa T. (2007) Subcutaneous administration of lactone form of simvastatin stimulates ectopic osteoinduction by rhBMP-2. *Oral Dis*. 13(2):228-233.
138. Zhang Y., Zhang R., Li Y., He G., Zhang D., Zhang F. (2011) Simvastatin

augments the efficacy of therapeutic angiogenesis induced by bone marrow-derived mesenchymal stem cells in a murine model of hindlimb ischemia. *Mol Biol Rep*.

139. Fiedler J., Etzel N., Brenner R.E. (2004) To go or not to go: Migration of human mesenchymal progenitor cells stimulated by isoforms of PDGF. *J Cell Biochem*. 93(5):990-998.
140. Gurtner G.C., Werner S., Barrandon Y., Longaker M.T. (2008) Wound repair and regeneration. *Nature*. 453(7193):314-321.
141. Kumar A., Salimath B.P., Stark G.B., Finkenzeller G. (2010) Platelet-derived growth factor receptor signaling is not involved in osteogenic differentiation of human mesenchymal stem cells. *Tissue Eng Part A*. 16(3):983-993.
142. Zhang Y., Shi B., Li C., Wang Y., Chen Y., Zhang W., Luo T., Cheng X. (2009) The synergetic bone-forming effects of combinations of growth factors expressed by adenovirus vectors on chitosan/collagen scaffolds. *J Control Release*. 136(3):172-178.
143. Anusaksathien O., Jin Q., Zhao M., Somerman M.J., Giannobile W.V. (2004) Effect of sustained gene delivery of platelet-derived growth factor or its antagonist (PDGF-1308) on tissue-engineered cementum. *J Periodontol*. 75(3):429-440.
144. Tokunaga A., Oya T., Ishii Y., Motomura H., Nakamura C., Ishizawa S., Fujimori T., Nabeshima Y., Umezawa A., Kanamori M., Kimura T., Sasahara M. (2008) PDGF receptor beta is a potent regulator of mesenchymal stromal cell function. *J Bone Miner Res*. 23(9):1519-1528.
145. Sun H.H., Qu T.J., Zhang X.H., Yu Q., Chen F.M. (2012) Designing biomaterials for in situ periodontal tissue regeneration. *Biotechnol Prog*. 28(1):3-20.
146. Chen F.M., An Y., Zhang R., Zhang M. (2011) New insights into and novel applications of release technology for periodontal reconstructive therapies. *J Control Release*. 149(2):92-110.